Memoirs of the School of Engineering, Nagoya University
Vol.46, No.2 (1994)

STUDY OF RADIOACTIVE NUCLIDES

Toshio KATOH, Kiyoshi KAWADE, Susumu AMEMIYA
and Hiroshi YAMAMOTO

Department of Nuclear Engineering

(Received November 1, 1994)

Abstract

Study of radioactive nuclides has been done. The radioactive elements were produced through the fast neutron irradiation, thermal neutron irradiation, charged particles irradiation and gamma-ray irradiation. The decay properties of produced radioactive nuclei were investigated by measuring beta-rays and gamma-rays. Decay schemes were constructed for these radioactive nuclei and many new excited levels were proposed from the results of the decay studies. Discussions concerning the nuclear structure was given on the basis of these newly proposed decay schemes. The methods of measurement of radioactive elements were applied for the measurements of cross sections of nuclear reactions. Study of nuclear reactions induced by the 14 MeV neuttrons become important from the view point of the fusion reactor technology. The 14 MeV neutrons due to the D-T burning in the fusion reactor cause activation of surrounding materials. The measurement of the cross sections of 14 MeV neutron reactions, therefore, is important to evaluate the effects of this activation. Then, the cross sections were measured. Cross section measurements of nuclear transmutation of fission products by thermal neutrons were also measured by using the activation method. The management of transuranium elements and fission products (nuclear waste) are important problem for the development of nuclear power technology. The transmutation of nuclear waste is one of method of the managements. Then, the measurement of cross sections of the transmutation reactions were designed. The values of cross sections were newly obtained.

Contents

1. Introduction

Since the radioactivity was discoverd by A. H. Becquerel in 1896, it has been one of the most important research subject in basic and applied physics. Radiations from the radioactive nuclei have been studied and became powerful tools for the study of nuclear properties. In the applied field, the radiations and radioactive elements have been used for various field of science and technology, such as improvement of material properties, use as tracers, monitors for trace element analysis and so on.

This paper describes research activity done at Department of Nuclear Engineering, Nagoya University in the field of Nuclear Physics and applied use of radioactivities.

2. Production of Radioactive Nuclides

Radioactive nuclides can be produced through various nuclear reaction processes. We produced them through reactions caused by fast neutron irradiation, thermal neutron irradiation, charged particle irradiation and gamma irradiation.

2. 1 Production of Radioactive Nuclides by Fast Neutron Irradiation

The fast neutron irradiations were performed by using a Van de Graaff accelerator and a 14 MeV neutron generator at Department of Nuclear Engineering, Nagoya University, by OCTAVIAN (an intense neutron irradiation facility) at Osaka University and by the Fast Neutron Source Facility (FNS) at Japan Atomic Energy Research Institute (JAERI).

The irradiation by the Van de Graaff accelerator at the Department of Nuclear Engineering, Nagoya University were made by using fast neutrons produced through a d-Li reaction on a Li target[1]. Deuteron beam accelerated by the Van de Graaff to 2 MeV causes the neutron producing reaction on a Li target. Improvement of the target cooling system combined with the selection of lithium metal as target materials made it possible to obtain a high flux neutron.

The Li target was fablicated by a simple melt-coating method since the uniformity of the target was not required for our experiments but high flux neutron was necessary. The target was prepared just before experiments and immediately installed into a vacuum system of the accelerator tube because the metalic lithium is chemically unstable. A thin target cooling system was developed to minimize the distance between the target and samples to be irradiated, which must be placed as close as possible to the neutron source. The cooling efficiency is another point to be considered. Then, relation between the relative neutron flux and the distance between the sample and the neutron target was studied. Based on this study, a target holder with 5.0 mm thick cooling system, as shown in Fig. 1, was devised. A thin vinyl sheet 0.1 mm thick was used as a water seal between the target and the cooling system.

The copper backing plate for the lithium target was directly cooled from the backside with water flowing at about 2 ℓ/min, which sufficed to remove 1 kW of heat generated from the target. The neutron flux from this target system was measured by gold foil activation method. A 20 cm^3 Ge(Li) detector, of which absolute detection efficiency was calibrated, was utilized to observe the 411.8 keV gamma-ray emitted from ^{198}Au and the 355.7 keV gamma-ray from ^{196}Au. The gold foils were irradiated at a distance of 12 mm from the target. The radioactive nuclei of ^{198}Au and ^{196}Au were produced through reactions ^{197}Au(n,γ)^{198}Au and

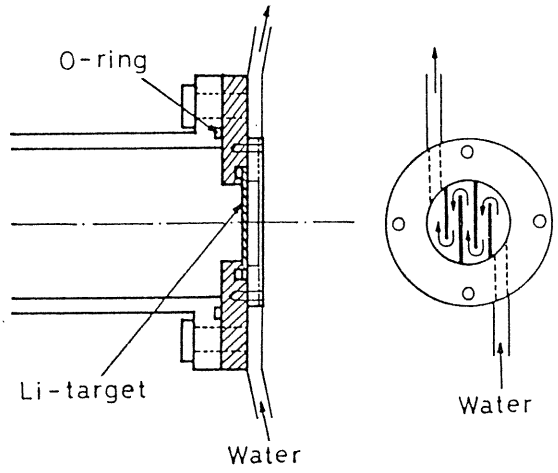

Fig. 1. Cooling system of 5 mm thick neutron target.

Table 1. Fast neutron fluxes measured at 12 mm in forward direction from targets, obtained by (d,n) reaction on lithium metal and tritium target.

Target material	Deuteron energy (MeV)	Fast neutron flux $\phi_f(n/cm^2 \cdot sec \cdot \mu A)$
Lithium metal	2.0	$(4.5 \pm 0.6) \times 10^6$
Tritium	0.75~1.0	$(4.8 \pm 0.6) \times 10^6$

$^{197}Au(n,2n)^{196}Au$, respectively. A tritium target, producing monochrome 14 MeV neutron, was used for comparison. The results of flux measurements with the present target system are shown in Table 1.

The irradiation with intense fast neutron flux from OKTAVIAN facility[2] at Osaka University was made by using a rotating tritium target.

OKTAVIAN consists of a high current deuteron beam accerelator with some special provisions for maintaining a high D^+ atomic ratio for D-T neutron production, highly effective water cooled rotating solid Ti-T target with the radius of 20 cm for continuous neutron supply, and a nanosecond pulse beam supply system with a small air cooled solid Ti-T target. The details of the facility is described in Ref. 2. The operation condition of the machine is as follows. The beam energy is 300 keV, maximum D^+ beam current at the rotating target is 20 mA, and the current for daily use 10 mA. The amount of tritium in the rotating target is 800 Ci/piece. The continuous D-D neutron yield is 3×10^{10} n/s and the continuous D-T neutron yield 3×10^{10} n/s. Fig. 2 shows the layout of the accerelator and the rotating target system.

The fast neutron source at FNS is also a high current deuteron beam accelerator with a rotating Ti-T target.

A fast neutron automatic activation system[3] was developed to produce and measure short-lived radioactive nuclei. The system was installed at the Van de Graaff accerelator at Nagoya University. The system consists of a Van de Graaff, a pneumatic transfer system, a gamma-ray detection system and a control system. All the process steps of the activation analysis, such as irradiation, transfer of the sample and measurement of gamma-rays are carried out in automatic sequence, governed by a programmed control system. The sample is transferred through a pneumatic tube between the irradiating position and the measuring station with pressurized gas. The transfer speed is determined by the pressure of the propelling gas and was 30 m/s at 2 kg/cm^2. The production and analysis of short-lived nuclei, such as ^{207m}Pb(half-life; 0.797 s), of half-lives below 1 s. were successfully performed with this system. The specified elements could be selectively analyzed by prescribing suitable intervals for irradiation, cooling and measurement.

2. 2 *Production of Radioactive Nuclides by Thermal Neutron Irradation and On-line Mass Separation of the Radioactive Elements*

Thermal reactors at Research Reactor Institute of Kyoto University, Japan Atomic Energy Research Institute and Rikkyo University were used for thermal neutron irradiation of samples. Operation condition of each reactor is described in the section of experimental

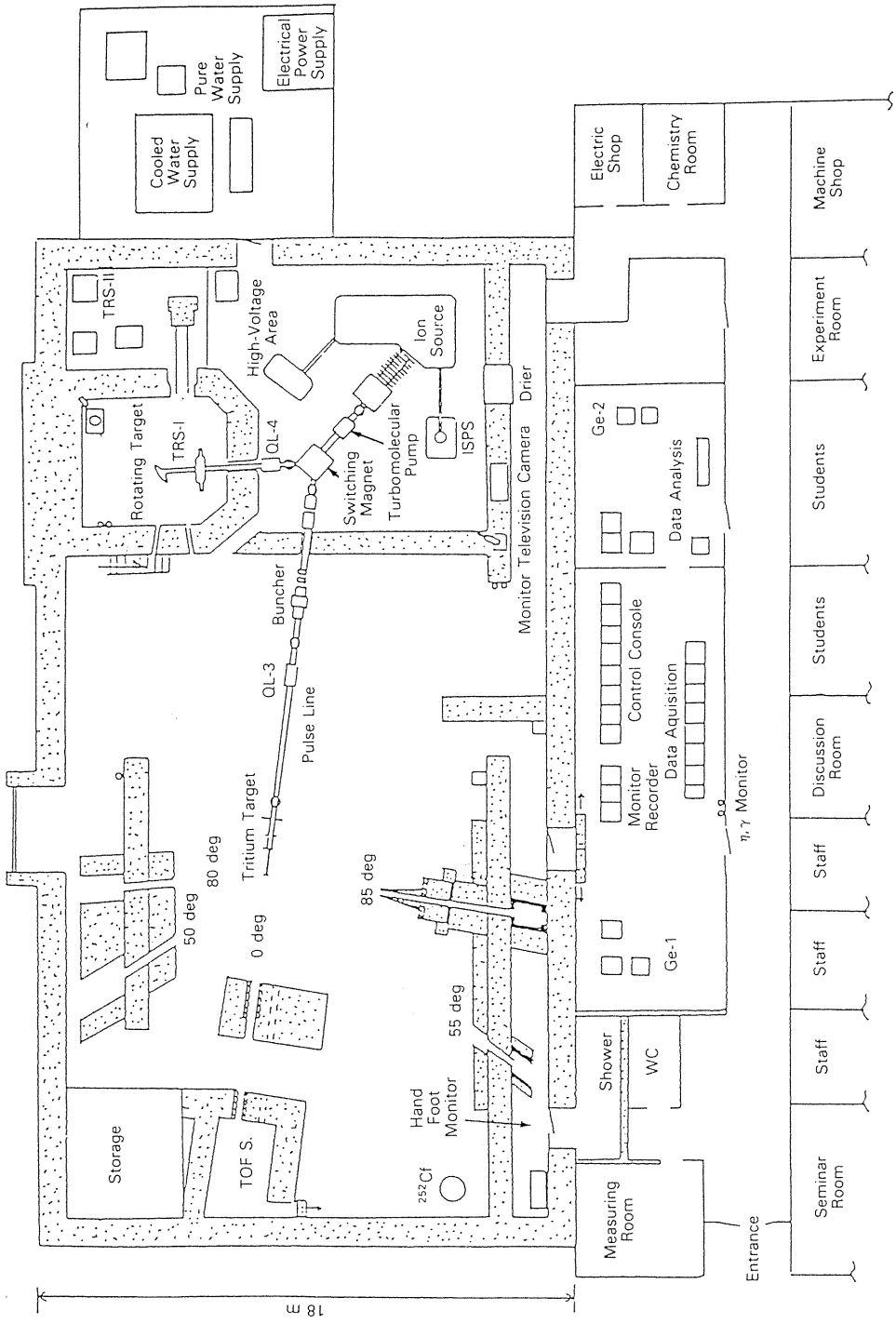

Fig. 2. Layout of OKTAVIAN.

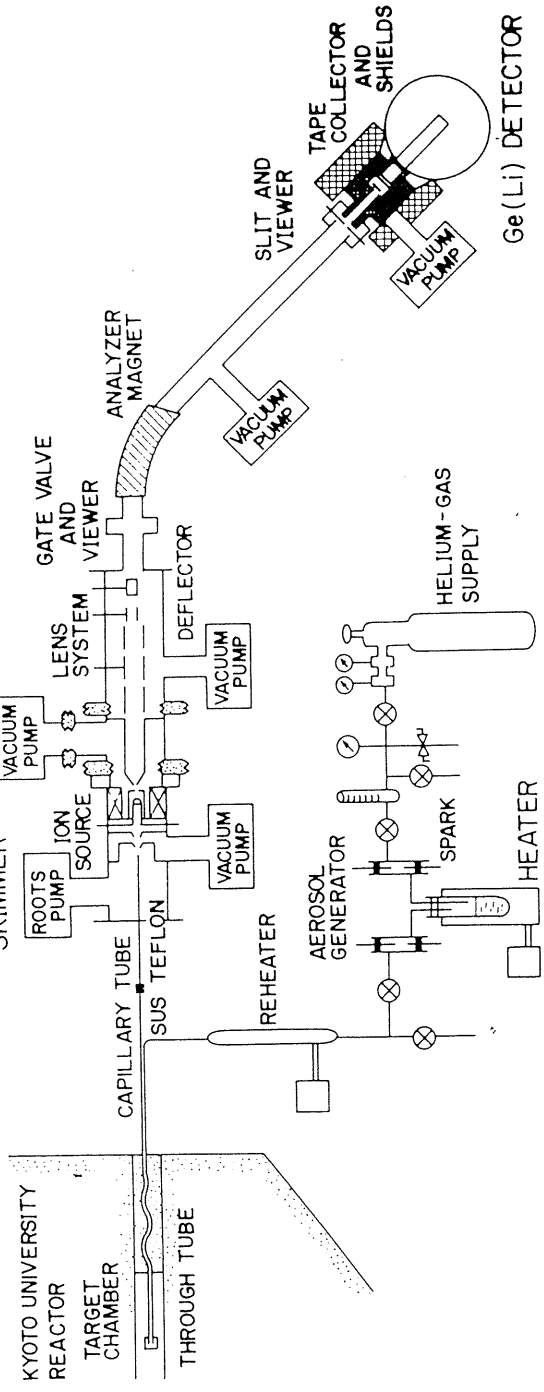

Fig. 3. Schematic diagram of a He-jet type ISOL at Kyoto University Reactor.

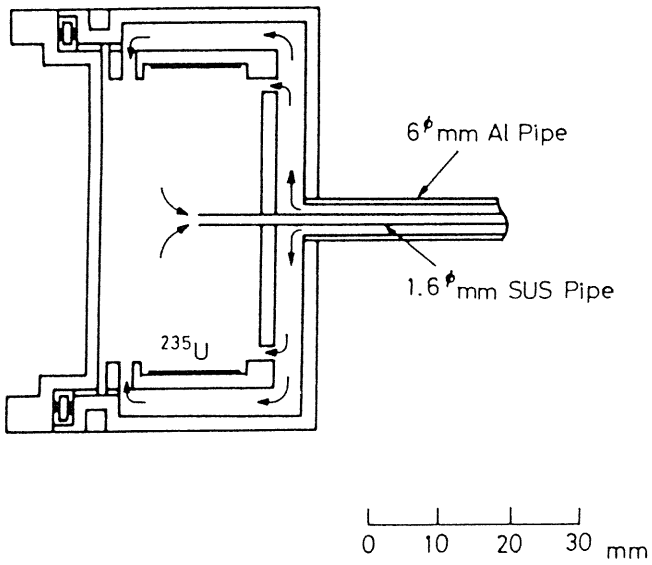

Fig. 4. A cross sectional view of ^{235}U target chamber.

procedure. Some elements were produced at the National Reactor Tesing Station, Idaho, U.S.A. and at Oak Ridge National laboratory, U.S.A.

A helium jet type on-line isotope separator (ISOL) was constructed[4),5)] at the Kyoto University Reactor (KUR) for the study of short-lived fission products. A schematic diagram of the ISOL system is shown in Fig. 3. A 93% enriched ^{235}U target material in the form of uranium oxide was electrodeposited on a 0.1 mm thick aluminum backing plate. The weight and thickness of the ^{235}U target material were 9.0 mg and 0.5 mg/cm^2, respectively. The target chamber is of a cylindrical shape, 44 mm inner diameter and 23 mm inner length, the open end of the capillary tube being located at the center. A cross sectional view of the target chamber is shown in Fig. 4. The target chamber can be moved along the inner tube of the through-tube facility of KUR so that the neutron flux at the target chamber is adjustable from 10^{10} n/cm^{2}s to 3×10^{12} n/cm^{2}s. Fission products produced in the target chamber is transferred to the ion source of the ISOL by using pressurized helium gas. The aerosol particles, which carry the fission products, are generated by heating DOP to 130°C or diffusion pump oil. The fission products transferred from the target chamber to the ion source of ISOL are ionized by using a Nielsen-type or a modefied hollow cathode type ion source. With the Nielsen-type ion source, the elements having low melting points were found to be ionized with moderate efficiency.

Typical ionization efficiencies were 0.44% for Te and 2.4% for iodine. A hollow cathode type ion source was constructed to ionize the elements having higher melting points. This ion source can ionize alkali elements with about 40% efficiency, working in a surface ionization mode. The ionized activities are extracted from the ion source and are focused in a parallel beam by accerelating and focusing electrodes. The parallel beam enters an analyzer magnet after passing through vertical and horizontal deflection plates. The parrallel beam is doubly focused at a distance of 120 cm from the exit of the magnet. The mass resolution measured with a 1 mm slit using a Xe beam was about 600 as shown in Fig. 5. Contamination

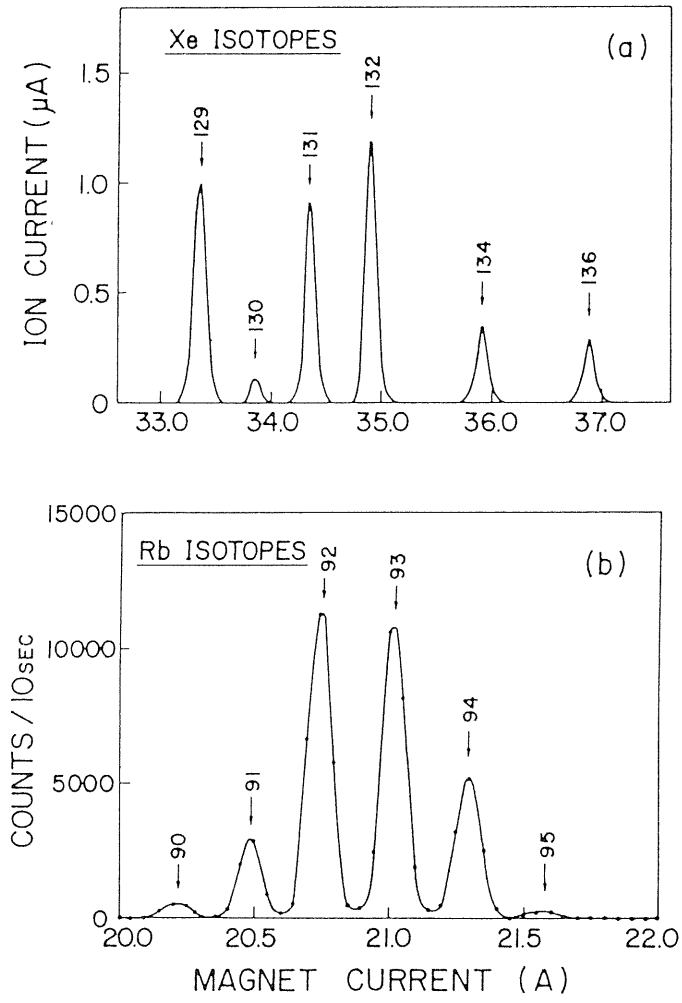

Fig. 5. Mass spectra of stable xenon isotopes (a) and rubidium isotopes (b) from fission products.

of gamma-rays from the neighbouring isotopes was usually negligibly small. The transport efficiency through a capillary has been measured to be about 60% for the ^{235}U fission products. The sweep time of fission products through a target chamber and the transit time through a capillary have been measured and were about 4 s and 1 s, respectively.

2. 3 Production of Radioactive Nuclides by Charged Particles and Gamma Irradiation

Cyclotrons at Institute for Nuclear Study, University of Tokyo and at Osaka University, and a linear accelerator at Research Reactor Institute of Kyoto University were used for production of radioactive elements. The cyclotrons were used for charged particle reaction and the linear accelerator for gamma irradiation.

3. Precise Measurement of Gamma-Ray Intensities

It is necessary to obtain precise value of gamma-ray intensities, because they will be fundamental data for activation analysis of trace elements, measurement of activation cross section, study of nuclear structure, non destructive nuclear fuel investigation, measurement of nuclear burn-up rate and other applied use of radioactive elements.

We designed experiments[6] to determine gamma-ray intensities in the energy region from 280 keV to 2750 keV with accuracies less than 1%. The points of remark in our precision measurements are as follows:

1) Reliable calibration gamma-ray sources were prepared. Disintegration rates of these sources were determined with an accuracy less than 0.5% by means of the coincidence method, and gamma-ray intensities per decay are accurately evaluated.

2) Careful measurements and data analyses were performed. We took care of gamma-ray absorption, the distance between the source and the detector, the position of the source on the source holder plate, the dead time of the electronic systems, the sum effect and the background subtraction.

3) Various kinds of efficiency curves were examined to fit our observed efficiencies and the best fitted function was decided. Gamma-ray efficiency measurements and relative intensity measurements of ^{56}Co, ^{88}Y and ^{207}Bi were perfomed with two Ge(Li) detector systems at Nagoya University and Hiroshima University. Relative intensities of ^{110m}Ag and ^{134}Cs were measured at Hiroshima University. Relative intensities and intensities per decay of gamma-rays from ^{56}Co, ^{88}Y, ^{110m}Ag, ^{134}Cs and ^{207}Bi were obtained.

Eight kinds of standard sources and four kinds of cascade gamma-ray sources were used for efficiency calibration. These sources are ^{24}Na, ^{90}Nb, ^{88}Y, ^{52}Mn, ^{60}Co, ^{22}Na, ^{46}Sc, ^{54}Mn, ^{134}Cs, ^{108m}Ag, ^{85}Sr and ^{203}Hg. A part of solution of about 1 μCi was mounted and dried up on the center of a plastic capsule (5 mmϕ). Radioactivity concentration of the solution for the standard sources was determined by means of the β-γ or X-γ coincidence methods. The amount of mounted solution was measured with a precision balance (Mettler M5) by means of the pycnometer method. Ten standard sources were made for each nuclide. Five were used at Nagoya and the other five at Hiroshima. The standard sources of ^{54}Mn and ^{88}Y used at Nagoya were also measured at Hiroshima. The average intensity of five sources of Nagoya is in good agreement with that of Hiroshima. It was inconvenient to make standard souces from short-lived nuclides of ^{24}Na, ^{52}Mn and ^{90}Nb. Hence, these nuclides were used for relative intensity calibration as cascade gamma-ray sources. The ^{24}Na nuclide was produced by the reactor at Rikkyo University, the sources ^{52}Mn and ^{90}Nb by the cyclotron at Institute for Nuclear Study, University of Tokyo. A ^{108m}Ag source was prepared from a ^{110m}Ag solution, which was supplied from Oak Ridge National Laboratory, of more than ten years old. The ^{108m}Ag source was very useful as a cascade gamma-ray source. All the sources were mounted on plastic capsules of 25 mm in diameter.

The coincidence measurement was performed with a box-type 4π counter and two 76 mmϕ × 76 mm NaI(Tl) detectors at the Electrotechnical Laboratory in Tokyo. The reliability of this system was already established by the international intercomparison measurement[7].

Gamma-ray intensity measurements were performed with a Canberra closed-end type Ge(Li) detector at Nagoya and an ORTEC true coaxial type Ge(Li) detector at Hiroshima. Linear amplifiesrs ORTEC 451 and ORTEC 472 were used at Nagoya and Hiroshima, respectively, and a biased amplifier, ORTEC 408 at Nagoya. Data taken at Nagoya were analyzed with FACOM 230-25 at Rikkyo University, Tokyo and data analyses at Hiroshima were performed with PDP11/05.

Measurements were performed by means of a similar method at Nagoya and Hiroshima. First, detector efficiencies were determined with eight kinds standard sources, ^{22}Na, ^{46}Sc, ^{54}Mn, ^{60}Co, ^{85}Sr, ^{88}Y, ^{134}Cs and ^{203}Hg, and one cascade gamma-ray source, ^{108m}Ag, in the energy range between 279 and 1836 keV. Secondly, the region was extended to 2754 keV with a cascade gamma-ray source ^{24}Na at Nagoya and with sources, ^{24}Na, ^{52}Mn and ^{90}Nb at Hiroshima.

After the efficiency measurements, relative gamma-ray intensities of ^{56}Co, ^{88}Y, ^{207}Bi, ^{110m}Ag and ^{134}Cs were measured.

In these measurements, special care were taken for the absorption effect of the cover of plastic cases and aluminum case of the Ge(Li) detector, the accuracy of source-to-detector-distance, efficiency dependence on the azimuthal angle of source position, and the counting loss due to the dead time and the chance coincidence sum of the detector system.

The recorded gamma-ray spectra were analyzed by computers. In the analyses, the background subtraction, subtraction of close lying gamma peaks and integration of peak area were carefully done. An example of subtraction of the Compton background is shown in Fig. 6. The source was placed 20 cm from the detector case to avoid the sum effect. However, the sum effect cannot be neglected. The observed spectrum of ^{108m}Ag indicates that the sum effect is of the order of 0.1%.

For the correction of the sum effect, the total efficiency curve was determined by using single gamma-ray emitters, ^{54}Mn, ^{85}Sr and ^{203}Hg. The angular correlation was considered for the correction of true coincidence sum effect. The chance coincidence sum was measured by using the single gamma-ray of ^{137}Cs. The ratio of chance coincidence sum peak to the 662 keV peak of ^{137}Cs was 4×10^{-5}.

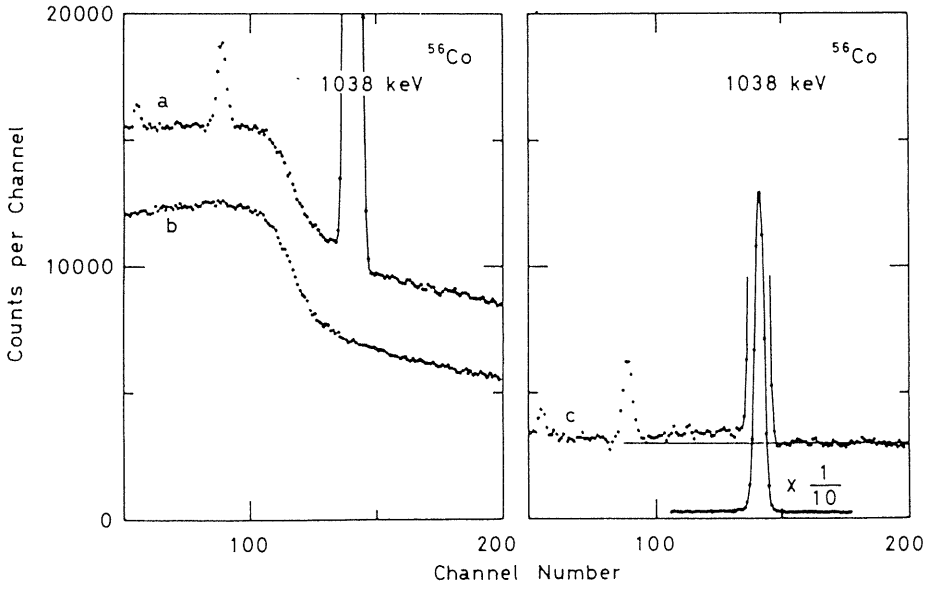

Fig. 6. Subtraction of the steep Compton background for the ^{56}Co 1038 keV gamma-ray;
(a) the gamma-ray spectrum
(b) adjusted Compton part of ^{22}Na
(c) Subtracted spectrum

It is well known that the efficiency curve for the Ge(Li) detector plotted in the logarithmic scale is almost linear in the energy region of 0.2–2 MeV and the curve in the semi-logarithmic scale becomes linear in the region higher than 2 MeV. We need much more accurate efficiency curve for the precision intensity determination. The detector efficiencies (ε) were obtained from the integrated peak counts of standard sources, the source strengths, the evaluated intensities per decay and the sum correction.

We tried to fit the obtained data to various curves. The best fitted curves are

$$\varepsilon = a_1 exp(b_1 E) + a_2 exp(b_2 E) + a_3 exp(b_3 E), \tag{1}$$

$$\varepsilon = exp\left[\frac{a_{-1}}{E-b} + a_0 + a_1(E-b)\right] \tag{2}$$

where a_i and b_i are parameters and E the gamma-ray energy. These two curves are shown in Fig. 7. By using χ^2 test, the best fit curves together with previously reported curves were investigated. It was found that the eq. (1) was the best, and that of eq. (2) was the next.

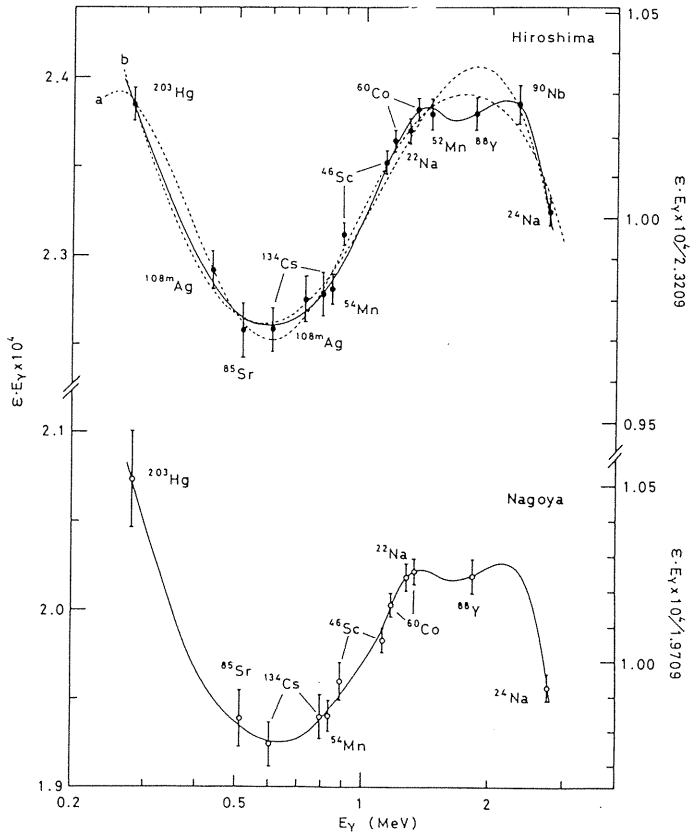

Fig. 7. Efficiency curves taken at Hiroshima and Nagoya. The solid curves indicate the final efficiency curves.

In Fig. 7, the high energy part seem very strange shape, and a curve shown by the following equation fits well.

$$\varepsilon = a_1 exp(b_1 E) + a_2 exp(b_2 E) \tag{3}$$

Finally, the acuracy of the efficiency was determined as errors of 0.3–0.5%. Precision measurement of relative gamma-ray intensities were performed by using these efficiency curves. Experimental results of ^{88}Y and ^{207}Bi are shown in Table 2 and Table 3, respectively.

Table 2. Relative intensities of ^{88}Y gamma-rays.

Gamma-ray energy (keV)	Relative intensities (%)				
	Present			Schötzig et al. [1]	Ardisson et al. [17]
	Hiroshima	Nagoya	Average		
898.0	94.3 ± 0.3	94.5 ± 0.4	94.4 ± 0.3	94.9 ± 0.5 a)	92.0 ± 0.7 a)
1836.1	100.0 ± 0.3	100.0 ± 0.5	100.0 ± 0.3	100	100

a) Obtained from intensities per decay.

Table 3. Relative intensities of ^{201}Bi gamma-rays.

Gamma-ray energy (keV)	Relative intensities (%)				
	Present			Rao et al. [18]	Jardine [19]
	Hiroshima	Nagoya	Average		
569.7	100.0 ± 0.4	100.0 ± 0.4	100.0 ± 0.4	100	100
897.3	0.122 ± 0.013		0.122 ± 0.013	0.150 ± 0.015	0.14 ± 0.02
1063.6	75.88 ± 0.25	75.51 ± 0.26	75.79 ± 0.25	78.7 ± 4.0	75.5 ± 2.3
1442.2	0.132 ± 0.005		0.132 ± 0.005	0.150 ± 0.015	0.15 ± 0.02
1770.2	7.026 ± 0.029		7.026 ± 0.029	7.5 ± 0.4	6.95 ± 0.20

The multi-gamma-ray source is very useful as a relative intensity calibration source. Therefore, gamma-ray intensities were measured for ^{56}Co, ^{110m}Ag and ^{134}Cs. Results are shown in Ref. 6. Relative gamma-ray intensities of five useful nuclides were determined with errors of 0.3–0.5%. Intensities per decay for ^{56}Co, ^{88}Y, ^{110m}Ag, ^{134}Cs and ^{207}Bi were calculated from the relative intensities and experimental or theoretical internal conversion coefficients by using the well-established decay schemes. The results are shown in Table 4.

The same method was extended to the energy region of 90 to 300 keV. The relative intensities and the intensities per decay of gamma-rays of ^{75}Se and ^{133}Ba, which are valuable for calibration, were obtained[8]. Relative intensities of these nuclides were obtained with estimated errors less than 1% for strong gamma-rays. Gamma-ray intensities per decay were also extracted. Results are shown in Ref. 8.

Table 4. Intensities per decay of ^{56}Co, ^{88}Y, ^{110m}Ag, ^{134}Cs, ^{207}Bi gamma-rays.

Nuclide	Gamma rays		Nuclide	Gamma rays	
	Energy (keV)	Intensity per decay (%)		Energy (keV)	Intensity per decay (%)
^{56}Co	486.5	0.061 ± 0.010	^{110m}Ag	706.7, 708.3	16.70 ± 0.12
	733.6	0.193 ± 0.012		744.3	4.73 ± 0.03
	787.8	0.305 ± 0.013		763.9	22.26 ± 0.13
	846.8	99.920 ± 0.007		818.0	7.33 ± 0.05
	896.6	0.095 ± 0.018		884.7	72.6 ± 0.4
	977.4	1.434 ± 0.016		937.5	34.33 ± 0.20
	996.9	0.129 ± 0.014		997.2	0.134 ± 0.005
	1037.8	14.15 ± 0.07		1085.4	0.062 ± 0.012
	1089.1	0.05 ± 0.03		1117.5	0.039 ± 0.005
	1140.3	0.131 ± 0.021		1125.7	0.036 ± 0.007
	1160.0	0.095 ± 0.014		1163.2, 1164.9	0.075 ± 0.011
	1175.1	2.239 ± 0.014		1251.0	0.023 ± 0.007
	1198.8	0.051 ± 0.009		1300.0	0.024 ± 0.008
	1238.3	66.0 ± 0.3		1334.4	0.141 ± 0.005
	1272.0	0.025 ± 0.008		1384.3	24.25 ± 0.14
	1335.5	0.130 ± 0.006		1421.0	0.037 ± 0.003
	1360.2	4.262 ± 0.022		1475.8	3.992 ± 0.024
	1442.7	0.172 ± 0.007		1505.0	13.03 ± 0.07
	1462.3	0.084 ± 0.006		1562.3	1.028 ± 0.008
	1640.4	0.070 ± 0.011		1592.6	0.0209 ± 0.0012
	1771.4	15.48 ± 0.07		1629.7	0.0058 ± 0.0010
	1810.7	0.656 ± 0.023		1775.4	0.0063 ± 0.0010
	1963.8	0.706 ± 0.011		1783.4	0.0097 ± 0.0010
	2015.4	3.024 ± 0.017		1903.5	0.0149 ± 0.0014
	2034.9	7.76 ± 0.04	^{134}Cs	563.1	8.37 ± 0.05
	2113.3	0.363 ± 0.007		569.2	15.40 ± 0.08
	2213.0	0.389 ± 0.008		604.7	97.64 ± 0.06
	2276.1	0.124 ± 0.007		795.8	85.52 ± 0.05
	2373.5	0.083 ± 0.011		801.8	8.68 ± 0.04
	2523.8	0.068 ± 0.011		1038.4	0.984 ± 0.006
	2598.6	16.95 ± 0.08		1167.7	1.783 ± 0.010
	2657.4	0.021 ± 0.006		1365.0	3.001 ± 0.017
^{88}Y	898.0	93.7 ± 0.4	^{207}Bi	569.7	97.74 ± 0.03
	1836.1	99.24 ± 0.07		897.3	0.119 ± 0.012
^{110m}Ag	365.4	0.086 ± 0.018		1063.6	74.0 ± 0.3
	387.1	0.07 ± 0.03		1442.2	0.129 ± 0.005
	396.9	0.06 ± 0.03		1770.2	6.87 ± 0.04
	446.8	3.739 ± 0.027			
	620.4	2.803 ± 0.019			
	626.3	0.216 ± 0.013			
	657.8	94.54 ± 0.20			
	676.6, 677.6	10.48 ± 0.09			
	687.0	6.43 ± 0.06			

4. Study of Decay Properties of Radioactive Nuclides

Decay properties of radioactive nuclides have been studied. The properties are very important data for the study of nuclear structure and for the applied use of radioactive elements. We measured mostly properties of medium weight nuclei, which belong to the transitional region (from the spherical to the deformed shapes), and fission product nuclei, which are important for the study of reactor physics and engineering.

4. 1 *Decay of ^{179}Hf*

The decay property of ^{179}Hf have been studied by Morinaga and Takahashi and others[9]. However, there is still ambiguity and then measurement was performed[10]. The sources was prepared by irradiating 400 mg of HfO_2, enriched to 99% in mass 180 with 14 MeV neutron produced by a neutron generator at Department of Nuclear Engineering, Nagoya University. The ^{180}Hf targets were wrapped in polyethelene foils, irradiated for half a minute and sent through a pneumatic tube to a counting room. The flight time was about 3 s.

Sum spectra of gamma-rays from produced ^{179}Hf through ^{180}Hf(n,2n)^{179}Hf reaction were measured by a well type scintillation spectrometer. Decay of the gamma peaks seen in the spectra were followed and the half-life were determined as 19 ± 2 s. Energies of excited levels of ^{179}Hf were estimated from energies of gamma peaks of the observed spectra. The K internal comversion coefficient of the 161 keV transition was obtained by analyzing the gamma peak intensities by using intensity relation. Detail of the analysis is shown in Ref. 10. Obtained value of the internal conversion coefficient was 17 ± 2. The branching ratio of the K conversion process and gamma-ray emission of the 161 keV transition are 0.48 ± 0.05 and 0.029 ± 0.003, respectively. A theoretical K conversion coefficient for the 161 keV M3 transition of ^{179m}Hf was estimated and is 19. The obtained value was in good agreement with the theoretical one within the statistical error.

The E4 admixture was estimated from this conversion coefficient, and the mixing ratio(E4/M3) was 0.14 ± 0.14. The branching ratio of the E4 component estimated from Weisskopf estimate[11] is 0.002. The present mixing ratio is in good agreement with this branching ratio.

4. 2 *Decay of ^{154}Eu*

The relative conversion electron intensities of 16 transitions of ^{154}Eu were measured[12] in an iron free double focusing spectrometer at Vanderbilt University, U.S.A., to investigate the beta-vibrational levels of deformed nuclei[13)–17)]. The ^{154}Eu activity was obtained by irradiating high purity ^{153}Eu samples in a high flux reactor (MTR) at the National Reactor Testing Station, Idaho.

The K conversion coefficients of the nine strong transitions were measured by the internal-external conversion method[18], and multipole characteristics of these transitions were obtained.

The most striking features of the results of this study is the large conversion coefficients of the 534, 676, 681 and 692 keV transitions. The conversion electron intensities of the 676 and 692 keV transitions between the 4^+ and 2^+ levels of the beta vibrational band and the 4^+ and 2^+ levels for the ground state rotational band, respectively, show that they were about 90% E0 transitions. Transitions of 534 and 681 keV are assigned to be pure E0 transitions.

4. 3 *Electric Monopole Transition in ^{156}Gd*

Internal conversion spectra from the decay of ^{156}Eu were measured[19] at high resolution with an air-core beta-ray spectrometer[20] at Institute for Nuclear Study, University of Tokyo. The decay product is ^{156}Gd, and the nucleus ^{156}Gd with the neutron number 92 belongs to the transition region but is more strongly deformed from ^{154}Gd. The deviation from the Alaga rules[21] in the β-band are remarkable in ^{156}Gd and ^{154}Gd, and cannot be interpreted by the rotational-vibrational interaction with β-ground mixing and β-γ mixing. In the present work, more accurate measurements of conversion electrons from the decay of ^{156}Eu were carried out. The source of ^{156}Eu was produced through the double neutron capture process by irradiating separated ^{154}Sm (in the form of Sm_2O_3) with thermal neutrons of JRR-2 reactor at Japan Atomic Energy Research Institute (JAERI) at a flux of 1×10^{14} n/cm^{2}s and

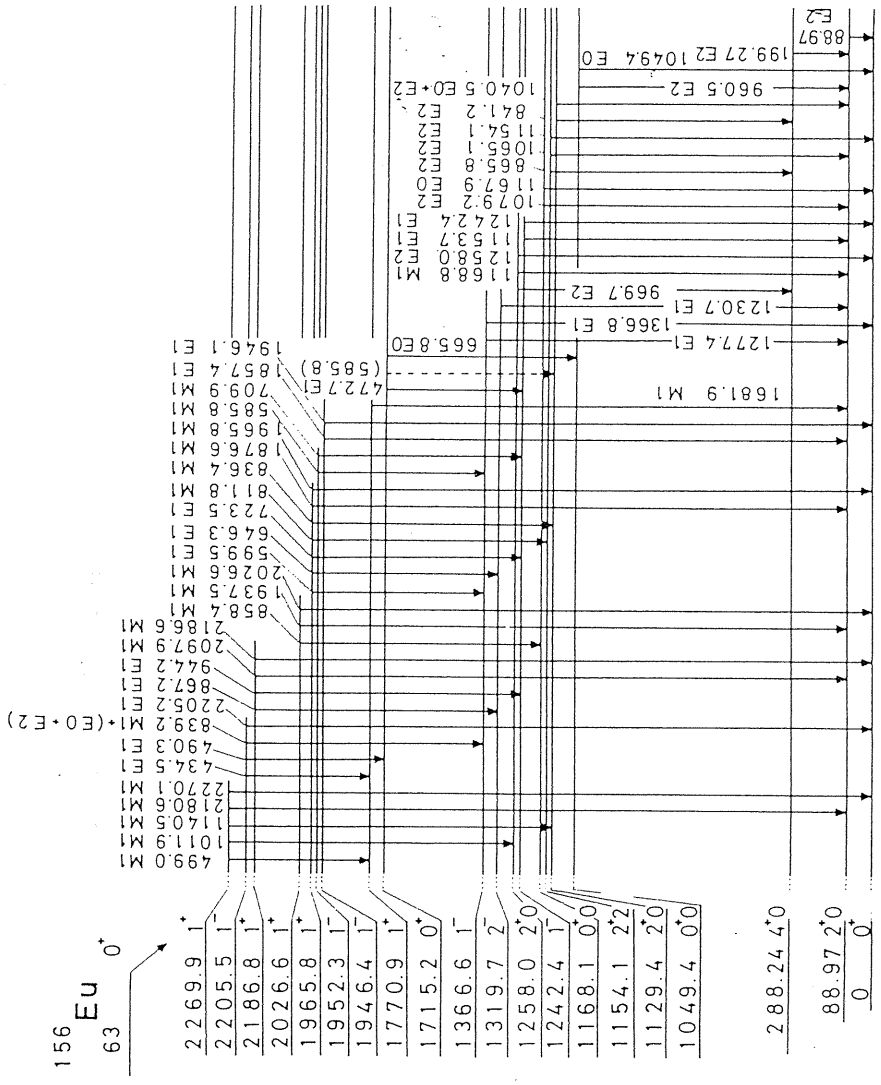

Fig. 8. A proposed decay scheme of ^{156}Eu.

3×10^{13} n/cm^{2}s. The process of the production is as follows; ^{154}Sm(n,γ)^{155}Sm → β decay → ^{155}Eu(n,γ)^{156}Eu. Then, ^{156}Eu can be produced from ^{154}Sm. Another irradiation of ^{154}Sm was also performed at Oak Ridge National Laboratory, U.S.A. with the thermal neutron flux of 1×10^{15} n/cm^{2}s. An ion exchange method was employed to separate the Eu fraction from the irradiated Sm_2O_3 samples. The separated carrier-free Eu activity was electro-deposited onto a 2.5 μm thick nickel foil to make beta-ray sources for an air-core double focusing beta-ray spectrometer[20]. Conversion electrons from the ^{156}Eu source were measured with the beta-ray spectrometer. A higher resolution setting of 0.03% was employed for separation of closely spaced doublet lines. Half-life of the ^{156}Eu was determined from the decay of conversion

electron peaks in the conversion electron spectrum and was 15.0 ± 0.1 day. Conversion electron peaks from ^{155}Eu activity, which were inevitably mixed in the separated Eu fraction, were identified by the decay measurement. Comparison of intensity ratio of measurements by three different sources was also used for separation of the ^{155}Eu peaks, since ratio of production depends on the neutron flux. Forty-seven K conversion lines were observed in the conversion electron spectrum above 248 keV. Among them, newly observed 12 conversion lines were consistent with data of gamma-ray measurements. Another one newly observed transition with energy of 665.8 keV was considered to be an electric monopole transition, since no peaks was found in the gamma-ray spectrum at the energy corresponding to this transition. Doublet lines at 1153 and 1168 keV were separated in this experiment. The line at 1153 keV consists of 1153.67 and 1154.08 keV lines and the line at 1168 keV consists of 1167.9 and 1168.8 keV lines. The multipolarity of the separated 1167.9 keV transition was E0. Our data were combined with recent gamma-ray data to deduce conversion coefficients for 47 transitions. Spins and parities of several levels were assigned or confirmed. Three 0^+ states at 1049.4, 1168.1 and 1715.2 keV were confirmed. Obtained decay scheme of ^{156}Eu (excited states of ^{156}Gd) is shown in Fig. 8. The β-ground mixing parameter of ^{156}Gd is obtained to be 0.014, while the β-γ mixing parameter 0.029 for the 2^+_β state and 0.005 for the 4^+_β state.

4. 4 Decay of ^{42}K, ^{76}As, ^{80m}Br and ^{152m}Eu

Decay of ^{42}K, ^{76}As and ^{80m}Br were studied for the purpose to give experimental data concerning the nuclear structure. Study of decay of ^{152m}Eu was done to confirm existence of a new level of ^{152}Sm.

Decay of ^{42}K: Decay of ^{42}K was studied[22] to investigate the nuclear structure of this nucleus in comparison with a theoretical prediction[23]. Powder of K_2CO_3 was rapped by a powder paper and encapsulated in a small polyethylene cylinder, and was irradiated for 1 min in a neutron flux of 2×10^{13} n/cm^{2}s at Kyoto University Reactor (KUR). The irradiated samples were sent to a experimental area by a pneumatic tube system. Gamma-ray measurement was carried out immediately after the irradiation without any chemical separation. Singles and coincidence spectra of gamma-rays emitted in the decay of ^{42}K were measured with a 24 cm^3 Ge(Li) detector and a 12.5 cm$\phi \times$ 10 cm NaI(Tl) scintillation counter. Peaks were seen in the spectrum taken by the Ge(Li) detector at 312.6, 899.7, 1021.2, 1524.6, 1920.8 and 2424.3 keV. A gamma-gamma coincidence spectrum shows peaks at the energy of 692.0 and 1228.0 keV as well as peaks seen in the single spectrum. These two gamma-rays have not been reported previously. A gamma-peak at 587 keV, which was reported previously[24], was searched, but was not observed above the background. The upper limit of this gamma-ray intensity against the intensity of the 899.7 keV gamma-ray was less than 0.7%. This upper limit was consistent with the calculated value of 0.4—0.6% where 4p-2h type deformation is taken into account. A proposed decay scheme including two new gamma-rays (692.0 and 1228.0 keV) are shown in Fig. 9.

Decay of ^{76}As: Decay of ^{76}As was investigated[25] by using a Ge(Li) detactor and Ge(Li)-NaI(Tl) coincidence methods. The purpose of the study is to search two phonon triplet states predicted by the vibrational model in excited states of ^{76}Se, decay product of ^{76}As. Natural arsenic (99.99%) was irradiated in neutron flux of 2×10^{13} n/cm^{2}s at Research Reactor Institute of Kyoto University (KUR) to produce ^{76}As. Gamma-ray measurements were carried out after cooling for 10 hours to eliminate effects of short-lived activities. Any chemical separation was not performed. Singles and coincidence spectra of gamma-rays from ^{76}As were measured with an ORTEC 20 cm^3 Ge(Li) detector system. The resolving power of the

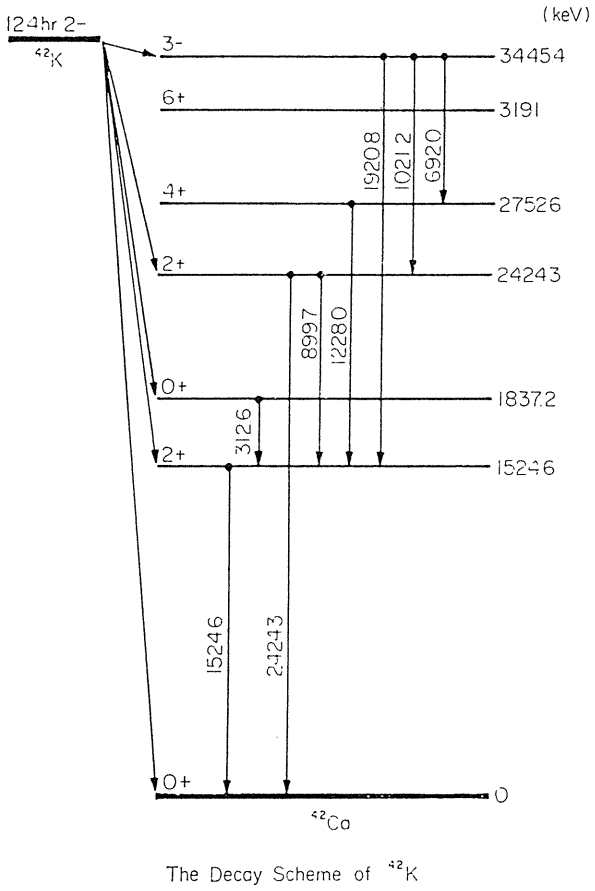

Fig. 9. A proposed decay scheme of ^{42}K.

detector was 3.0 keV at the full width at half maximum of the peak of 1332 keV gamma-ray of ^{60}Co. In the analysis of observed spectra, consideration for escape peaks and radioactive impurities were taken into account. Forty-eight gamma-rays were observed in the present experiment. Sixteen new gamma-rays were observed, about half of them were seen only in the coincidence spectrum and eleven of them were assigned in a proposed decay scheme. Two gamma peaks close lying around 560 keV were seen as shown in Fig. 10. The upper spectrum shows the spectrum in coincidence with the 560 keV gamma-peak, and the lower shows that with the 660 keV gamma-peak. The coincidence intensity of the 563.4 keV peak was reduced in the spectrum with the gate at 660 keV. This fact indicates that the 563.4 keV gamma-ray would be a transition from the second excited 0^+ state (see the decay scheme in Fig. 11). A decay scheme of ^{76}As proposed from this experiment is shown in Fig. 11. The 2026.4, 2348, 2365.1 and 2514 keV levels were newly found. Forty-one gamma-rays among 48 ones were definitely assigned in the decay scheme. The levels at 559.3, 1122.7, 1216.5 and 1331.4 keV have been explained as vibrational levels of ^{76}Se. The 559.3 keV level is a one-phonon state and the levels at 1122.7, 1216.5 and 1331.4 kEv levels are two phonon states. The 0_2^+ and 0_1^+

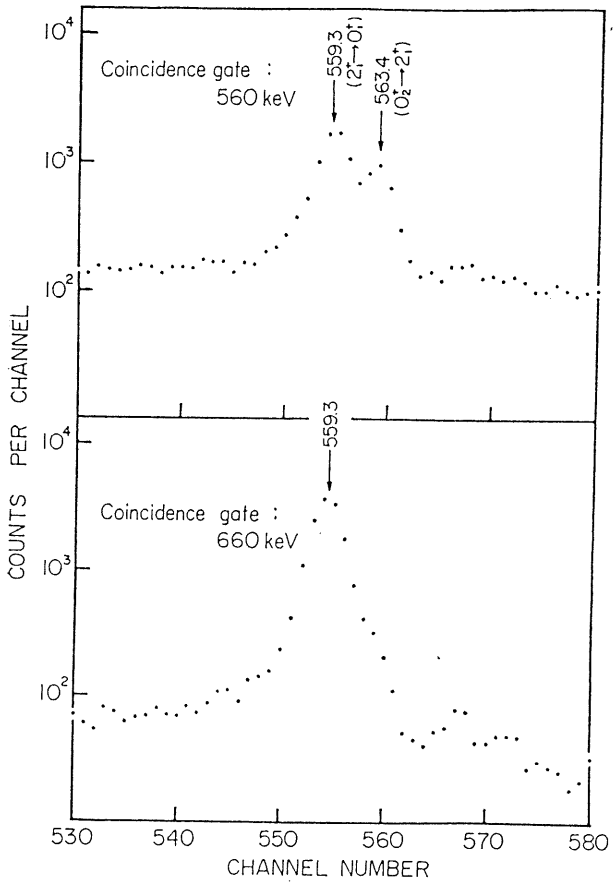

Fig. 10. Coincidence spectra near the 559 keV gamma peak.

levels of the two phonon states were observed in (p, p')[26], (d, d')[27] reactions and the coulomb excitation[28] experiments. The energies and intensities of gamma-rays from these levels were uncertain because the energies are very close to the energy of the gamma-ray (559.3 keV) from the first excited state.

In this experiment, the gamma-transition (563 keV) from the 0_2^+ state to 2_1^+ state was separated from the 559.3 keV transition. The energies of gamma-rays in this doublet peak were 563.4 ± 0.1 and 559.3 ± 0.1 keV and the relative intensity 1:33.4. The 772.1 keV gamma-ray, which has not been fixed in the decay scheme, was assigned as the gamma-ray from the 4_1^+ state to the 2_1^+ state, since this gamma-ray was not seen in the spectrum in coincidence with the 1220 keV gamma peak. Thus, two phonon triplet states of ^{76}Se were confirmed in the this study of the decay of ^{76}As. Energies and relative intensities which have relation with these levels were determined precisely and a decay scheme of ^{76}As was proposed more definitely. Three phonon levels of ^{76}Se were investigated and the 1691.2 and the 1787.8 keV levels were assigned as three phonn states.

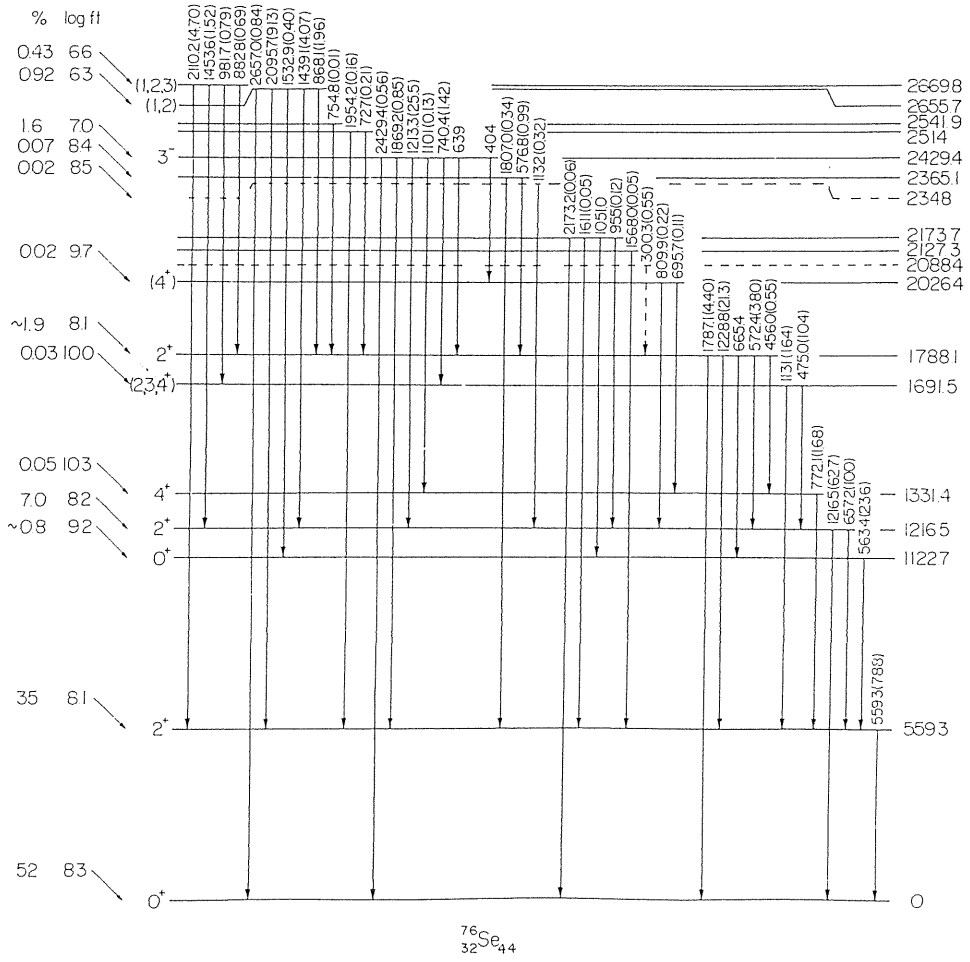

Fig. 11. Low lying levels of ^{76}Se.

Decay of ^{80m}Br: Decay of ^{80m}Br was investigated[29] to find triplet two phonon states of the spherical vibrational model in the excited states of ^{80}Se and ^{80}Kr. The half-lives of ^{80m}Br and ^{80}Br and beta-ray spectra were also studied. Sources of ^{80m}Br for the measurement were produced through thermal neutron irradiation of the sodium bromide in JRR-2 reactor at Japan Atomic Energy Research Institute (JAERI), of which neutron flux was 8×10^{13} n/cm^{2}s. The target was enriched to 99.75% in ^{79}Br. After the irradiation, chemical separation was performed. Sources for the half-life measurement of ^{80}Br were made by 5 MeV deuteron irradiation on natural lithium bromide. The deuteron beam was obtained from a cyclotron at Osaka University. Sources for the beta-ray spectrum measurement were made by the thermal neutron irradiation of the sodium bromide at Research Reactor Institute of Kyoto University. Decay of intensity of beta-ray which emitted from ^{80m}Br sources were followed by two G-M counters. Data were analyszed by means of the least square method for two components with a computer NEAC 2203. The values of the half-life determined from the two measurements

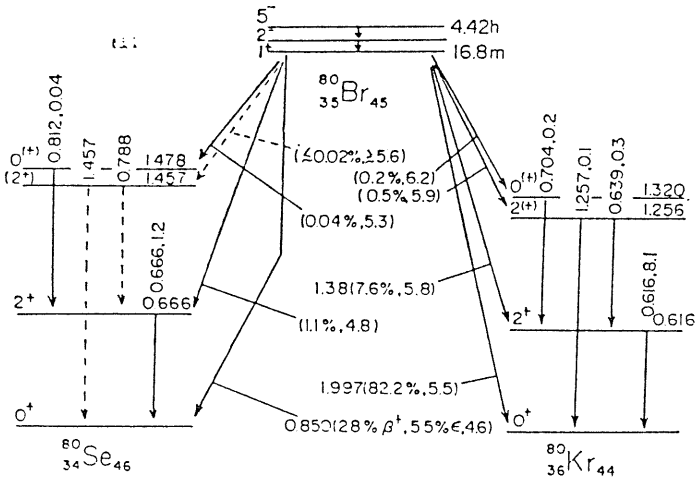

Fig. 12. A decay scheme of ^{80m}Br.

were 4.412 ± 0.010 and 4.424 ± 0.013 hour. The average value is 4.41 ± 0.10 hour where error includes the systematic error. The half-life of the ground state of ^{80}Br was also measured by a G-M counter. The computer analysis of the measured data give the half-lives of 16.88 ± 0.11 and 16.72 ± 0.11 min. and the average of the two measurements is 16.8 ± 0.1 min. The ^{80}Br decays through two ways such as β^+ decay to ^{80}Se and β^- decay to ^{80}Kr. Beta-ray spectra measurements were carried out using an 8 gap orange type beta-ray spectrometer of Osaka University. The resolving power and the transmission of the spectrometer were 1.0% and 3.0%, respectively. The analyses of the observed spectra gave the maximum energies of the beta-rays and relative intensities.

The maximum energy obtained of the β^+ ray was 0.850 ± 0.007 MeV and the relative intensity 2.8%, which gives a log ft value of 4.6. The β^- ray has two components and their maximum energies were 1.38 ± 0.02 and 1.997 ± 0.010 MeV. The relative intensities were 7.6 and 82.2%, respectively. Gamma-ray spectra were measured by using a 8 cm^3 coaxial type Ge(Li) detector and gamma-gamma coincidence spectra by using two 7.5 cmϕ × 7.5 cm NaI(Tl) scintillation counters. On the basis of observed gamma-ray data, a decay scheme of ^{80m}Br was proposed as is shown in Fig. 12. The 1.478 MeV 0^+ level of ^{80}Se and the 1.320 MeV 0^+ and 1.256 MeV 2^+ levels of ^{80}Kr were confirmed.

Decay of ^{152m}Eu: Decay of ^{152m}Em(9.3 h.) was studied[30] by using a Ge(Li) detector and a coincidence system with a NaI(Tl) scintillation counter and the Ge(Li) detector. Sources of ^{152m}Eu were produced by thermal neutron irradiation of ^{151}Eu, enriched to 96.7% in mass 151. A gamma-ray peak at 961.2 ± 0.6 keV was observed and this peak was definitely different from a gamma-ray of 964.0 ± 0.4 keV. The energy calibration of the detector and gain drift of the electronic circuit were carefully investigated. A new level, which is different from the 2^+ state at 1085.8 keV, was proposed at 1083.0 ± 0.6 keV in the level scheme of ^{152}Sm, and the 961.2 keV transition is emitted from this level. The probable spin and parity of the 1083.0 keV were estimated from the log ft value of the beta decay to this level and were 0^+ or 1^+. This result is consistent with the proposal of a new 0^+ state around 1091 keV[31]. If the

spin and parity of the 1083.0 keV is 0^+, this level is considered to construct a K = 0 band with the 2^+ state at 1292.0 keV.

4. 5 Decay of Radioactive Nuclei produced by using a 2 MeV Van de Graaff

Short-lived radioactive nuclides produced by fast neutron irradiation were studied to investigate neutron rich elements of medium weight region (transitional region). Decay data of this region are rather scarce than data of proton rich nuclides. Proton rich nuclides can be produced by charged particle reaction by using an accelerator. Nuclides which belong to the fission products can be obtained from fission products of uranium. However, the neutron rich nuclides in the medium weight region were hardly be produced. We planned to produce them through the (n, p) reaction by using 14 MeV neutron. Unfortunately, the formation cross section of these nuclides are usually small, and then, we designed a special target[1)] and transfer system[3)] as mentioned in Section 2.1. Our concern was concentrated in the short lived elements since their data were scarce and the intensities of the produced activity are relatively strong even the number of produced nuclei are small.

Decay of ^{148}Pr: The nucleus ^{148}Nd with 60 protons and 88 neutrons exists at the edge of the region of spherical shape. The addition of a pair of neutrons induces the transition from nuclear states of spherical character to the formation of states of a more non spherical equilibrium shape. Hence the nucleus is expected to exhibit some of properties being characteristic of transitional nuclei. An experiment[32)] was designed to establish the decay scheme of ^{148}Pr and to investigate the excited states of ^{148}Nd.

Radioactive sources of ^{148}Pr were obtained through the ^{148}Nd(n,p)^{148}Pr reaction by the fast neutron irradiation of sample $^{148}Nd_2O_3$ enriched to 95.44% in mass 148 with neutrons from a 2 MeV Van de Graaff accelerator at Nagoya University. Gamma-ray measurements were performed with a 23 cm^3 Ge(Li) detector with a resolving power of 2.5 keV at 1.332 MeV. A coincidence measurement was employed with a Ge(Li) detector and a 12.7 cmϕ × 10.2 cm NaI(Tl) scintillation counter. A 10 mm acrylic plate was put in front of the detectors to suppress beta-rays. The continuous beta-ray spectrum was investigated with a 5.08 cmϕ × 2.54 cm plastic detector. This detector together with a 7.62 cmϕ × 7.62 cm NaI(Tl) scintillation counter was also used for the β-γ coincidence measurement. A gamma-ray singles spectrum was obtained and impurity gamma peaks seen in the spectrum were distinguished by the values of energies and their half-lives. Decay of peaks were followed and peaks with a half-life of 2.3 ± 0.3 min were assigned as gamma peaks from ^{148}Pr. In order to follow the decay of the beta-ray spectrum, singles spectra were recorded in the eight sections of the multichannel analyzer for successive intervals of 70 s starting 1 min after the bombardment. Beta-rays in the observed spectra with the half-life of 2.3 ± 0.3 min was assigned to the beta-rays from the decay of ^{148}Pr. The end point energy of the beta-ray was determined from the Fermi-Kurie analysis and was 4.5 ± 0.2 MeV. The results of β-γ coincidence measurement indicates no direct beta-population of the ground state of ^{148}Nd. The half-life of the ^{148}Pr was measured. The decay of the 301.7 keV gamma peaks was followed by a Ge(Li) detector. A least square fit of the decay curve obtained gave a half-life of 2.28 ± 0.09 min. A decay scheme of ^{148}Pr was proposed as shown in Fig. 13. Four new levels were proposed and 20 gamma-rays were assigned in this decay scheme. The Q(β) value estimated from the proposed decay scheme was 4.8 ± 0.2 MeV. The 916.9(0^+), 1247.4(2^+) and 1682.4(4^+) keV levels are assigned as first three members of the quasi β-band predicted by Sakai[33)]. The 1170.5 keV level is assumed to be 2^+ member of the quasi γ-band[33)].

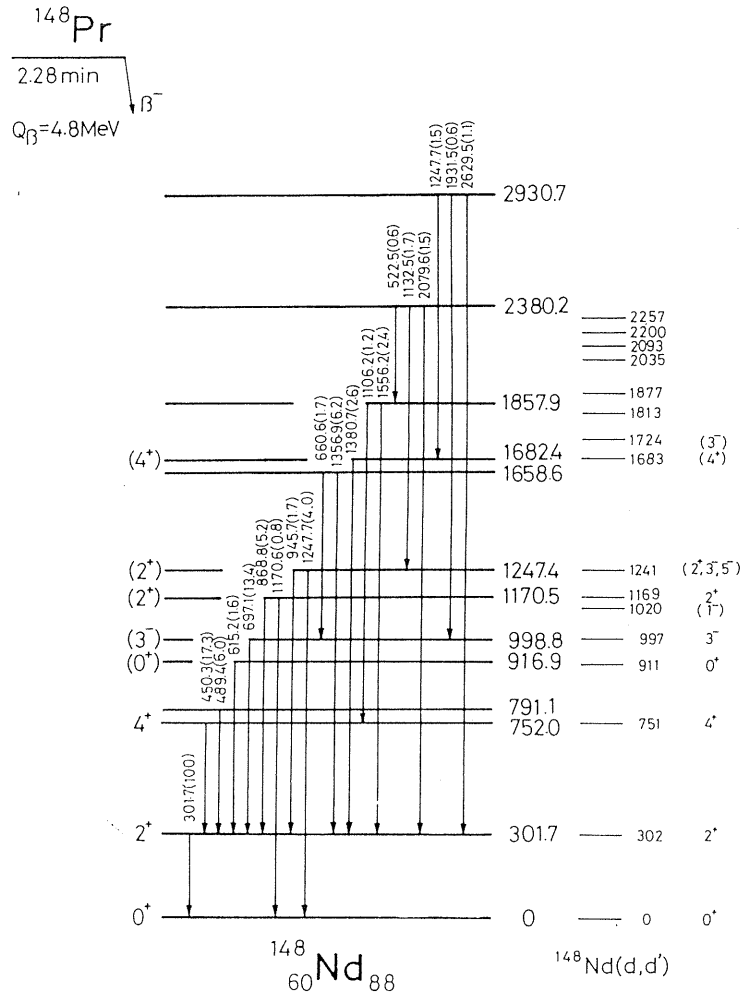

Fig. 13. A proposed decay scheme of ^{148}Pr.

Decay of ^{152}Pm: The ^{152}Sm nucleus with 62 protons and 90 neutrons is at the very beginning of the deformed rare-earth region. This is a fortunate situation, since the β- and γ-vibrational bands lie at lower excitation energies than the corresponding states of more rigid nuclei in the middle of the deformed rare-earth region due to the softness of this nucleus. The levels of ^{152}Sm have been studied by various methods, and some features on the levels are proposed. An experiment[34] was designed to confirm isomeric levels and to establish decay schemes of ^{152}Pm, and to investigate the excited states of ^{152}Pm more accurately. The radioactive sources of ^{152}Pm were obtained through the ^{152}Sm(n,p)^{152}Pm reaction by the irradiation of sample $^{152}Sm_2O_3$ enriched to 98.29% in mass 152 with 14.8 MeV neutrons from a 2 MeV Van de Graaff at Nagoya University. Interfering products due to the neutron reactions were ^{149}Nd, ^{151}Pm and ^{153}Sm and their gamma-rays are studied well. Gamma-rays from these elements

were distinguished in the observed spectra by the values of energies, relative intensities and their half-lives. The neutron flux on the target was 2×10^9 n/cm^{2}s with deuteron beam of 200 μA. The ^{152}Sm samples were irradiated 7.5 min, sent back to the counting station by a pneumatic transfer system, and the counting started 1 min after the end of the irradiation. The contribution of ^{16}N was reduced allowing a cooling time of 1 min. The bombardment and counting sequence was repeated to accumulate the satisfactory statistics. Gamma-ray spectra were measured by a 23 cm^3 Ge(Li) detector, and a coincidence system with a Ge(Li) detector and a 12.7cm$\phi \times$ 10.2 cm NaI scintillation counter was employed. The continuous β-spectrum was investigaed with a 5.08 cm$\phi \times$ 1.27 cm plastic detector. Gamma-ray peaks in the obtained spectra with half-lives of 4.30 $\pm$ 1.30 and 7.52 $\pm$ 0.80 min were assigned to the decay of ^{152}Pm isomers. A total of 129 gamma-trnsitions, including newly observed 96 gamma-rays have been observed. The beta-ray spectra were recorded in the four sections of the multichannel analyzer for successive intervals of 7.5 min starting 2 min after the irradiation to follow the component of ^{152}Pm. A Fermi-Kurie plot of the beta-ray of the spectrum of ^{152}Pm gave a maximum end point energy of 3.50 $\pm$ 0.10 MeV. Half-lives of 4.30 $\pm$ 0.37 min and 7.52 $\pm$ 0.08 min were obtained by following the decay of the sum of full energy peak area of the 695.9 and 841.4 keV gamma-rays, and that of the 1097.1 and 1437.5 keV ones, respectively.

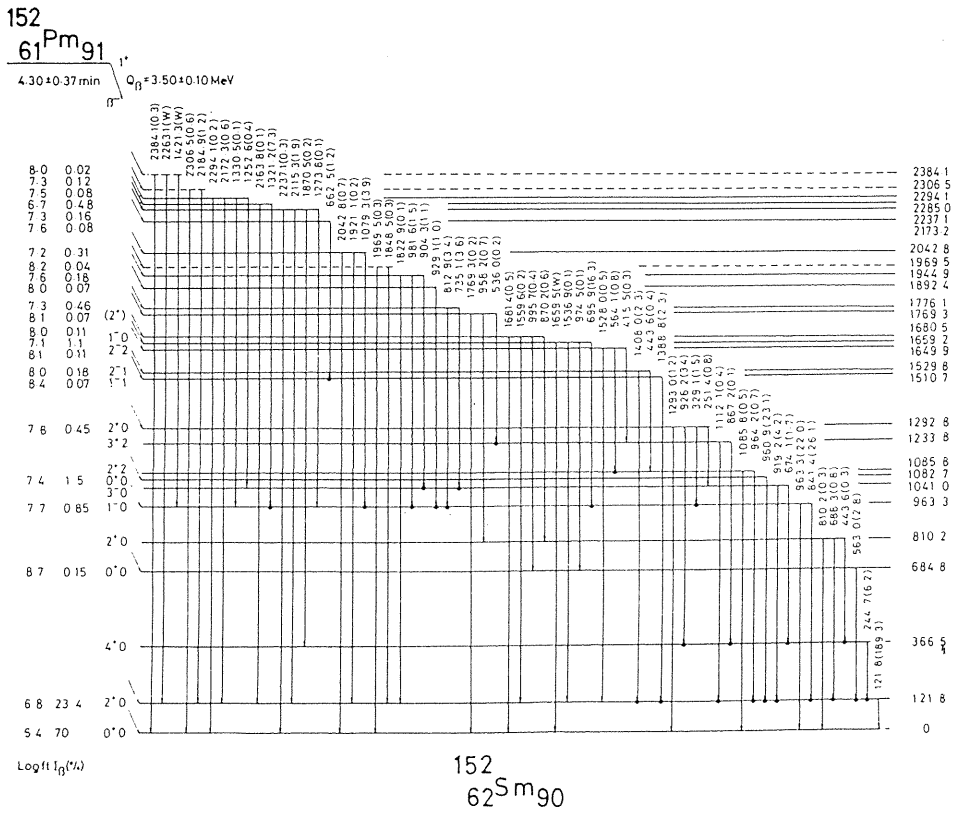

Fig. 14. A proposed decay scheme of 4.30 min ^{152}Pm.

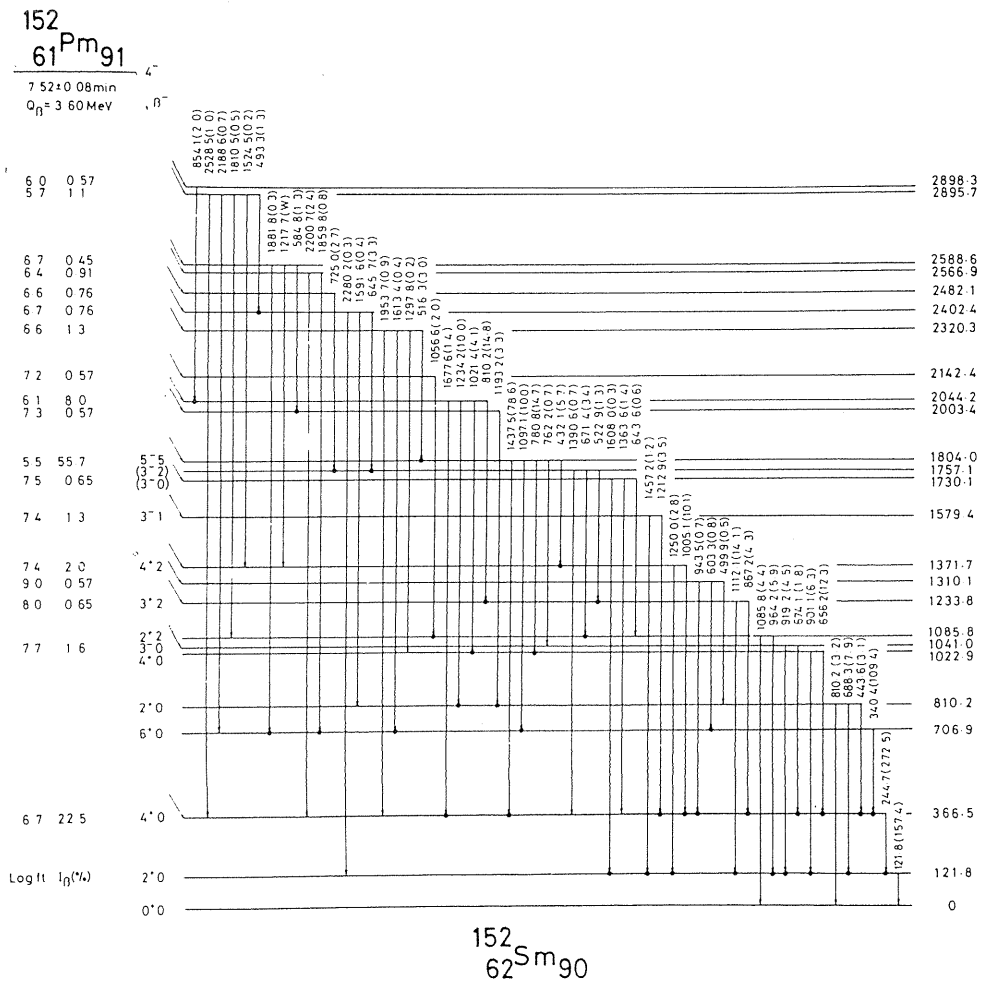

Fig. 15. A proposed decay scheme of 7.52 min ^{152}Pm.

Decay schemes of ^{152}Pm isomers were proposed from this experimental results as shown in Figs. 14 and 15. These decay schemes account for 108 gamma-rays of 129 gamma-rays observed in this experiment. Twenty-two levels were proposed for the first time. Most probable spin assignments of 1^+ and 4^- are proposed for the 4.30 and 7.52 min isomers, respectively. The results were discussed in terms of the unified model[35].

Decay of ^{154}Pm: The nucleus ^{154}Sm exists at the edge of the so-called region of deformed nucleus. This nucleus may exhibit some of the characteristic properties of transitional nuclei. Experiments[36] were proposed to confirm two isomers and to establish decay schemes of ^{154}Pm, and to investigate excited levels of ^{154}Sm more accurately. The radioactive sources were obtained through the reaction ^{154}Sm(n,p)^{154}Pm by the irradiation of samples $^{154}Sm_2O_3$ enriched to 99.54% in mass 154 with the 14 MeV neutrons produced by a 2 MeV Van de

Graaff of Nagoya University. Interfering products were ^{151}Nd, ^{155}Sm, ^{151}Pm and ^{153}Sm, and they were distinguished as mentioned before. The ^{154}Sm samples were irradiated by the fast neutron for 2.5 min, sent back to the counting station through the pneumatic system, and the counting started 45 s after the end of the irradiation. The contribution of ^{16}N was reduced by this cooling time. The irradiation and counting sequence was repeated to accumulate the satisfactory statistics. A 23 cm^3 Ge(Li) detector was used for the measurement of gamma-ray spectra, and a coincidence system with this Ge(Li) detector and a 12.7 cm$\phi \times$ 10.2 cm NaI(Tl) scintillation counter was employed. The continuous beta-ray spectrum was measured with a 5.08 cm$\phi \times$ 1.00 cm plastic detector. Seventy-five gamma-rays have been observed and 57 of them are assigned to the ^{154}Sm level scheme including four new levels. Decay schemes of two isomers of ^{154}Pm are proposed and shown in Fig. 16.

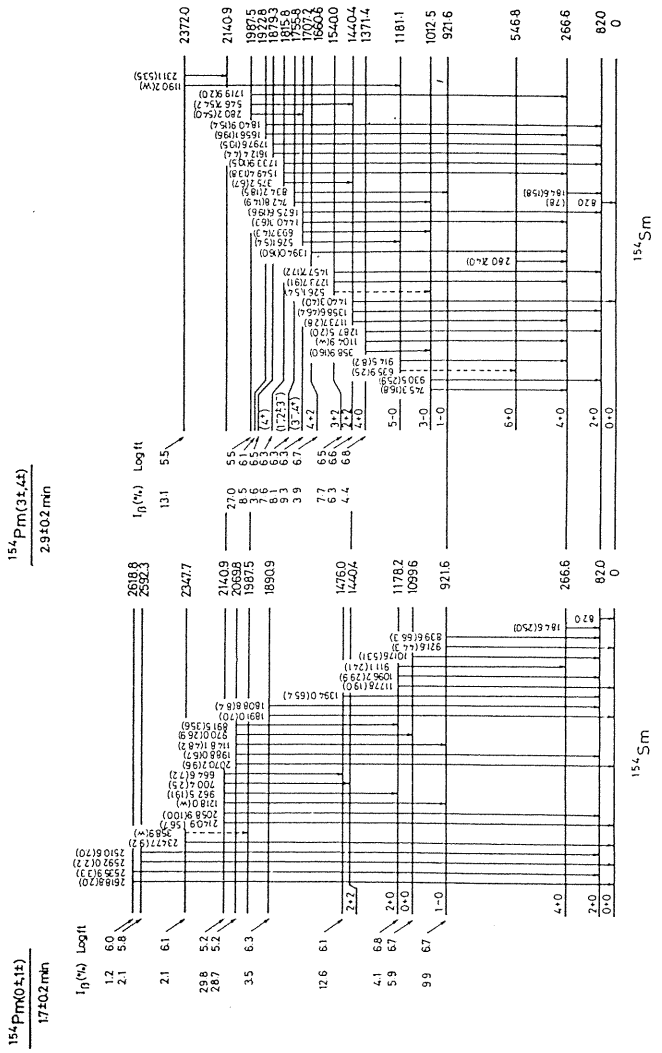

Fig. 16. Proposed decay schemes of ^{154}Pm isomers.

A Fermi-Kurie plot analysis of observed beta-ray spectrum indicated the presence of three beta-groups with end point energies of 3.0 ± 0.2, 1.9 ± 0.2 and 1.4 ± 0.3 MeV. To establish β-γ relations, β-γ coincidence measurements were performed. Beta-groups with end point energies of 2.4 ± 0.2 and 1.8 ± 0.2 MeV were seen in the coincidence spectra. Half-lives of 1.7 ± 0.2 min and 2.9 ± 0.2 min were obtained by following the decay of the sum of 2058.9 and 2140.9 keV photo peak area, and that of 1358.6 and 1440.3 keV ones, respectively. A Q_β value estimated from this experiment was 3.9 ± 0.2 MeV. Most probable spin assignment of $0^\pm$ or $1^\pm$ and $3^\pm$ or $4^\pm$ are proposed for the 1.7 ± 0.2 min and 2.9 ± 0.2 min ^{154}Pm, respectively. The properties of excited levels were discussed in comparison with the theoretical prediction by the Nilsson model[35].

Decay of ^{165m,g}Dy: The shape of ^{165}Ho nucleus is thought to be deformed. Experiments concerning the excited states of ^{165}Ho were designed by using the decay of ^{165m,g}Dy[37]. A Ge(Li) detector and a coincidence arrangement were employed to obtain accurate values of energies and intensities of gamma-rays in the decay of ^{165}Dy and ^{165m}Dy. The radioactive sources were produced through the ^{164}Dy(n,γ)^{165}Dy reaction by using the Van de Graaff accelerator at Nagoya University. The neutron produced by the reaction ^{7}Li(d,n)^{8}Be and thermalized with paraffin blocks irradiated the samples of ^{164}Dy. The thermal neutron flux at the samples was 6×10^8 n/cm^{2}s. A research reactor of Research Reactor Institute, Kyoto University was also employed for the production of ^{165m}Dy. Successive irradiation of 100 samples of natural dysprosium was carried out by using a pneumatic irradiation facility. Forty gamma-rays were observed in the gamma-ray spectrum with a Ge(Li) detector and a Ge(Li)-NaI(Tl) coincidence system. New gamma-rays were detected at the energies of 178 and 339 keV in the coincidence spectrum. Seven gamma-rays were seen in the gamma-ray spectrum of ^{165m}Dy. A delayed and a prompt coincidence measurements with the 361.8 keV gamma-ray were performed to confirm cascade relations. Decay schemes of ^{165}Dy and ^{165m}Dy were proposed, and the result shows the ground-band rotational levels at 94.6 and 209.6 keV.

Decay of ^{168}Ho: Decay of ^{168}Ho has been studied[38] with a Ge(Li), a NaI(Tl), and a plastic detectors in singles and in coincidence mode. Sources were prepared by the ^{168}Er(n,p)^{168}Ho reaction with 14 MeV neutrons from a 2 MeV Van de Graaff accelerator. Samples $^{168}Er_2O_3$ enriched in mass 168 of Er were used for the target. Thirty-three gamma-rays were observed and twenty-eight of them were assigned in a proposed decay scheme (see Fig. 17), including three new levels at 2192.7, 2254.4 and 2425.7 keV. The half-life of ^{168}Ho was measured to be 2.98 ± 0.09 min. The observation of a 1.92 ± 0.10 MeV beta group in coincidence with 821 keV gamma transition established the total beta decay energy as 2.74 ± 0.10 MeV. There is good agreement of beta decay branching ratios to the gamma-band with predictions from the adiabatic symmetric rotor model[39].

Decay of ^{170}Ho: Beta and gamma-rays emitted from the decay of ^{170}Ho isomers have been measured with a Ge(Li), a NaI(Tl) and a plastic detectors and decay character of these nuclei were studied[40]. The decay product ^{170}Eu is a strongly deformed nucleus. The ^{170}Ho activity was produced by irradiation of enriched $^{170}Er_2O_3$ with 14 MeV neutron generated from the Van de Graaff accelerator at Nagoya University. The fast neutron induced reaction ^{170}Er(n,p)^{170}Ho produced the ^{170}Ho sources. The beta-rays and gamma-rays were measured in singles and coincidence mode. Fifty gamma-rays have been observed and 36 of them were assigned to the ^{170}Er level scheme including 7 new levels at 1010.5, 1217.3, 1900.5, 1982.6, 2039.3, 2684.8 and 3606.2 keV. The most probable spin assignment of $1^\pm$ and $4^\pm$ were proposed for the 43 s and 2.8 min isomers of ^{170}Ho, respectively. Both Q_β values were almost

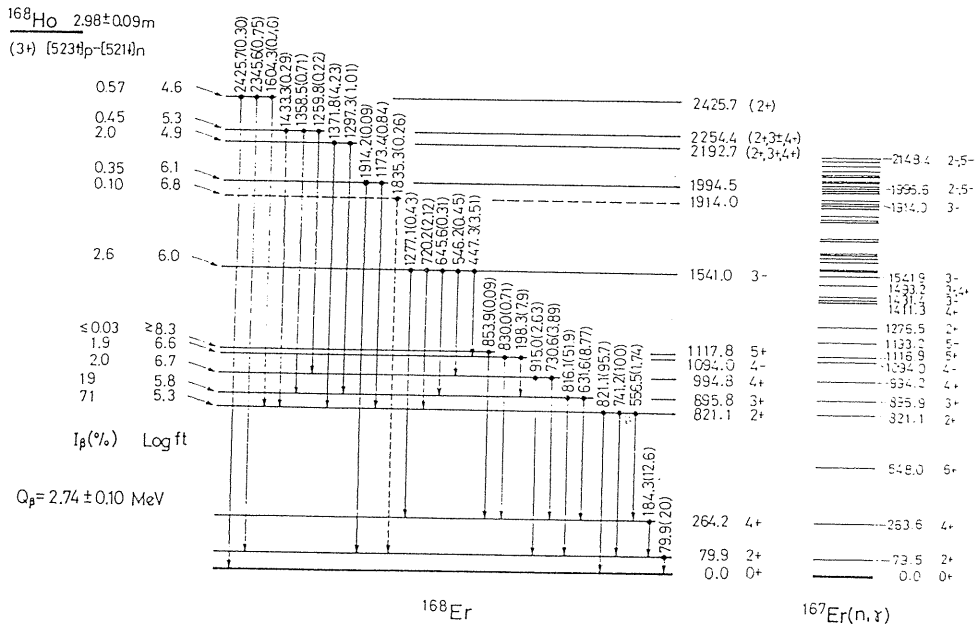

Fig. 17. A proposed decay scheme of ^{168}Ho.

same and 4.0 ± 0.2 MeV. The K = 0 assignment for the 2^+ state at 959.8 keV is proposed from the E2 branching ratio to the ground-state band. It is found that the relative B(E2) values from the γ-vibrational band can not be explained by a single value of the band mixing parameter. This discrepancy might well be explained by the presence of the $K=0^+$ band close to the γ-vibrational band.

4. 6 Decay of Radioactive Nuclei produced by Gamma-ray Irradiation

Decay of ^{178m,g}Lu and ^{162}Tb were studied by using 30 MeV bremsstrahlung produced by an electron linear accelerator of Research Reactor Institute of Kyoto University.

Decay of ^{178m,g}Lu: The decay properties of the ^{178}Lu isomers having spin-parities of 1^+ and 9^- were performed[41]. The decay product ^{178}Hf is a strongly deformed even-even nucleus, and it is interesting to study the level properties of this nucleus. Sources were prepared by the (γ, p) reaction on enriched ^{178}Hf samples. The beta- and gamma-rays were measured in both singles and coincidence modes by using a Ge(Li), a NaI(Tl) and a plastic detectors. Main interfering products in the irradiation were ^{179}Lu, ^{180m}Hf, ^{181}Hf and ^{177}Lu and their decay properties has been studied well. The counting started 15–20 min after the end of irradiation, thus reducing the contribution of ^{15}O. Forty gamma-rays were detected in the gamma-ray dpectrum, and 39 of them were assigned in the proposed decay scheme of ^{178m,g}Lu. Average values of 22.9 ± 0.4 min for the half-life of ^{178m}Lu and 28.1 ± 0.5 min for that of ^{178g}Lu were obtained by following the decay of 326 and 426 keV gamma-ray peaks and those of 1310 and 1341 keV gamma-ray peaks, respectively. The decay scheme includes 6 newly found levels of ^{178}Hf at the energies of 1174.4 ($I^\pi K = 2^+2$), 1199.3(0^-0), 1276.8(2^+0) and 1322.4(3^-2) keV in the ^{178g}Lu decay and 1364.04(9^-8) and 1601.6(10^-8) keV in the ^{178m}Lu

decay. The analyses of Fermi-Kurie plots gave the end point energies of beta transitions. The Q_β values were 2.05 ± 0.05 MeV for ^{178g}Lu and 2.25 ± 0.03 MeV for ^{178m}Lu. The most probable spin and parity assignment of 1^+ and 9^- were proposed for the ground and isomeric states of ^{178}Lu, respectively. There is reasonable agreement between the experimental beta-branching ratios from ^{178m}Lu to the 8^- band at 1147 keV and the Alaga rules[21]. The decay schemes of ^{178m,g}Lu proposed from this experiment are shown in Figs. 18 and 19. The spin-parity characteristics of the excited states of ^{178}Hf were discussed in comparison with the Nilsson orbitals. Two 8^- states at 1147 and 1479 keV have been known to be highly mixed states of $8^-\{[514\downarrow] + [624\uparrow]\}_{nn}$ and $8^-\{[404\downarrow] + [514\uparrow]\}_{pp}$ configuration. The ^{178m}Lu beta-decay rates to these two states also give evidence for the strong mixing: the observed log ft values of 5.24 ± 0.10 and 5.49 ± 0.10 indicate the slower allowed unhindered (*au*) and the faster allowed hindered (*ah*) transitions (systematical values are 4.5—5.0 for *au* and 6.0—7.5 for *ah*). Moreover, these values show that the 1147 keV state is mainly two quasi neutron configuration and that the 1479 keV state is mainly two quasi proton one.

Decay of ^{162}Tb: The level structure of the strongly deformed doubly even nucleus ^{162}Dy was studied through the decay of ^{162}Tb[42]. Sources were produced by the (γ, p) reaction on enriched ^{163}Dy samples. The beta- and gamma-rays were measured both in singles and coincidence modes with a Ge(Li), a NaI(Tl) and a plastic detectors. Main interfering products in the irradiation are ^{163}Tb and ^{165m,g}Dy, and their decay schemes are well known. For the

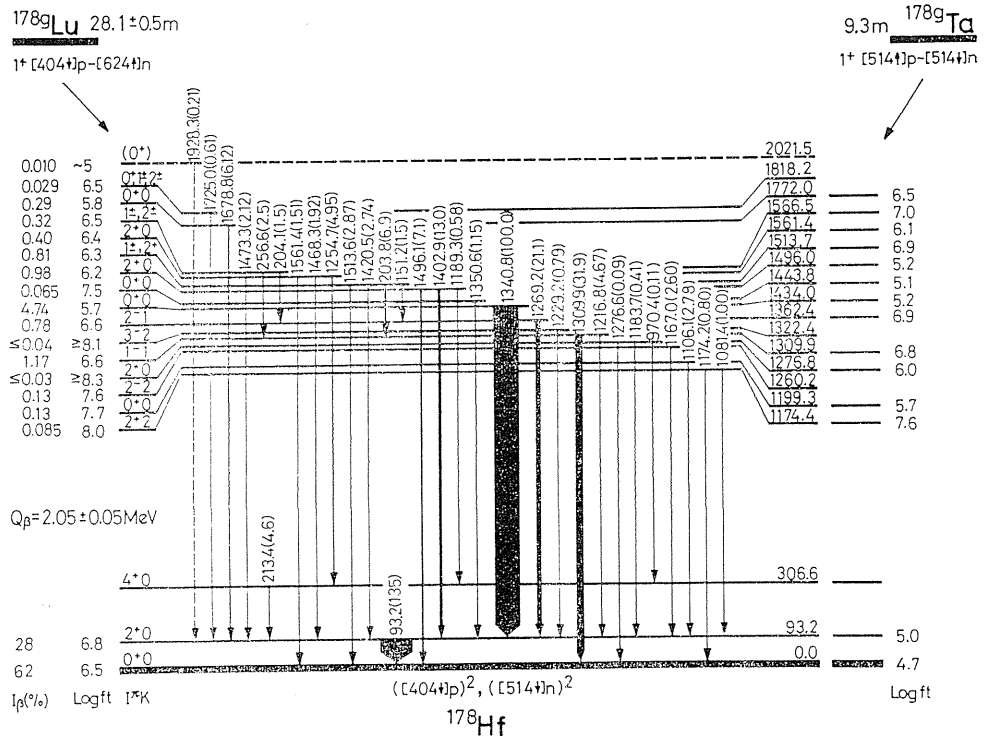

Fig. 18. A proposed decay scheme of 28.1 min ^{178}Lu.

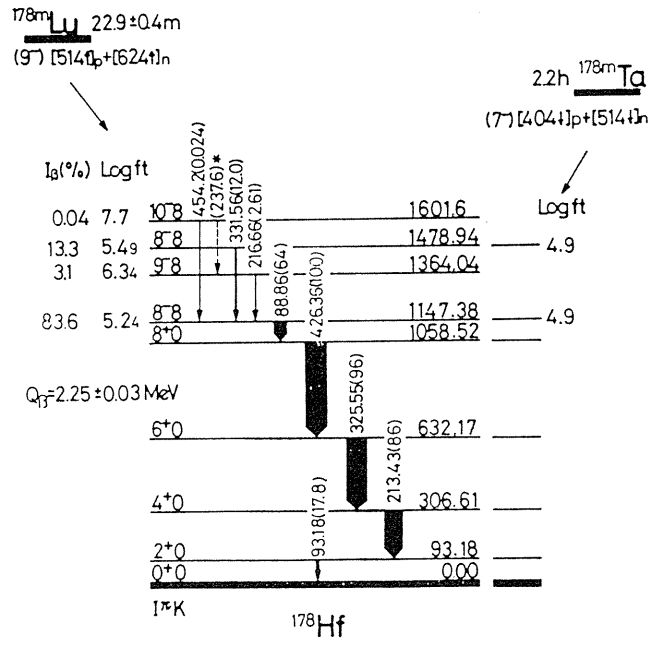

Fig. 19. A proposed decay scheme of 22.9 min ^{178m}Lu.

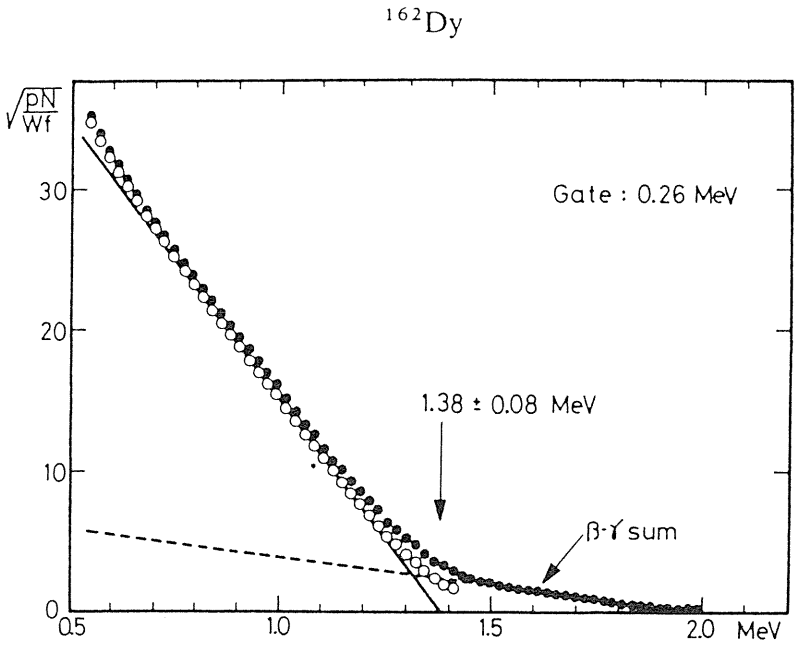

Fig. 20. A Fermi-Kurie plot of the ^{162}Tb β-ray spectrum in coincidence with the 0.26 MeV γ-ray peak.

assignment of the gamma-rays following the decay of ^{162}Tb, two successively recorded spectra were measured with the interval of 8 min. Thirty-five new gamma-rays were observed in addition to the previously known 12 gamma-rays[43]. A gamma-beta coincidence measurement was carried out to reduce the complicated contribution from beta-gamma summing effects and to determine the end point energy of the strong beta-branch of ^{162}Tb. A Fermi-Kurie plot analysis of the beta spectrum in coincidence with the 0.26 MeV gamma-ray peak gave an end point energy of 1.38 ± 0.08 MeV as shown in Fig. 20. The half-life of ^{162}Tb was determined by measuring 16 time sequential 1024-channel gamma-ray spectra with the interval of 150 s. The average value of 7.76 ± 0.10 min was obtained from a least-square fit of the decay data. A decay scheme of ^{162}Tb was proposed from this experiment and shown in Fig. 21. Total of 40 transitions were incorporated in the decay scheme comprising 17 excited states of ^{162}Dy. A spin parity assignment of 1^- is confirmed for the ground state of ^{162}Tb. Properties of the levels of ^{162}Dy was discussed in comparison with the Nilsson model.

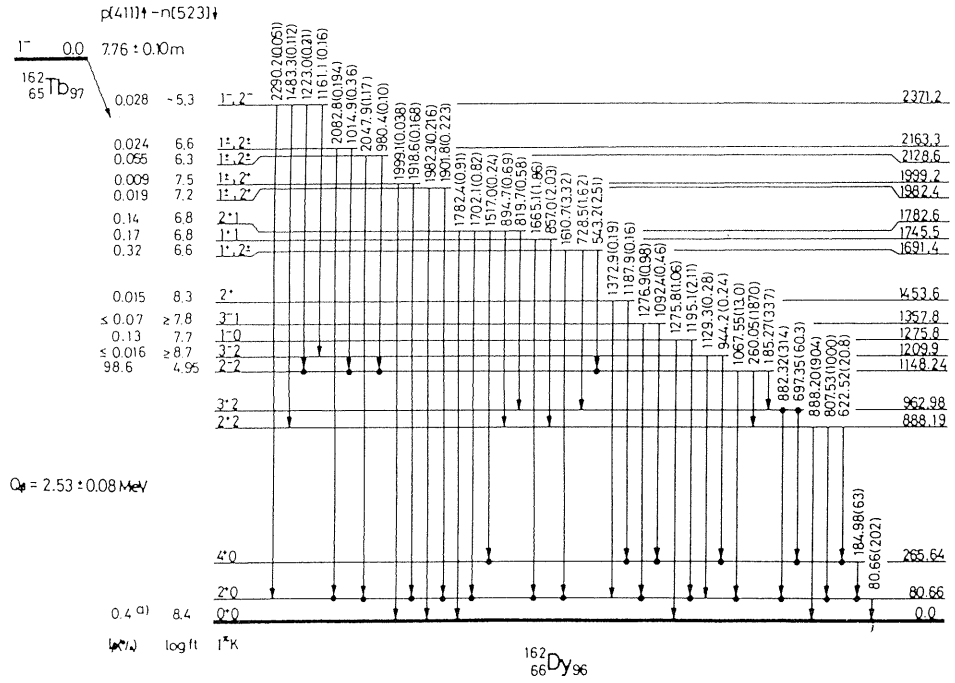

Fig. 21. A proposed decay scheme of 7.76 min ^{162}Tb.

4. 7 *Decay of Fission Products produced by Thermal Neutron Irradiation on ^{235}U and separated by the Paper Electrophoresis*

Study of fission product nuclei were performed to obtain decay data for evaluation of the decay heat of reactors and for the study of nuclear structure of the transitional region. Experiments were carried out mostly by using TRIGA-II reactor at Rikkyo University. Radioactive sources were prepared from fission products of ^{235}U. A small amount (about 30 $\mu\ell$) of

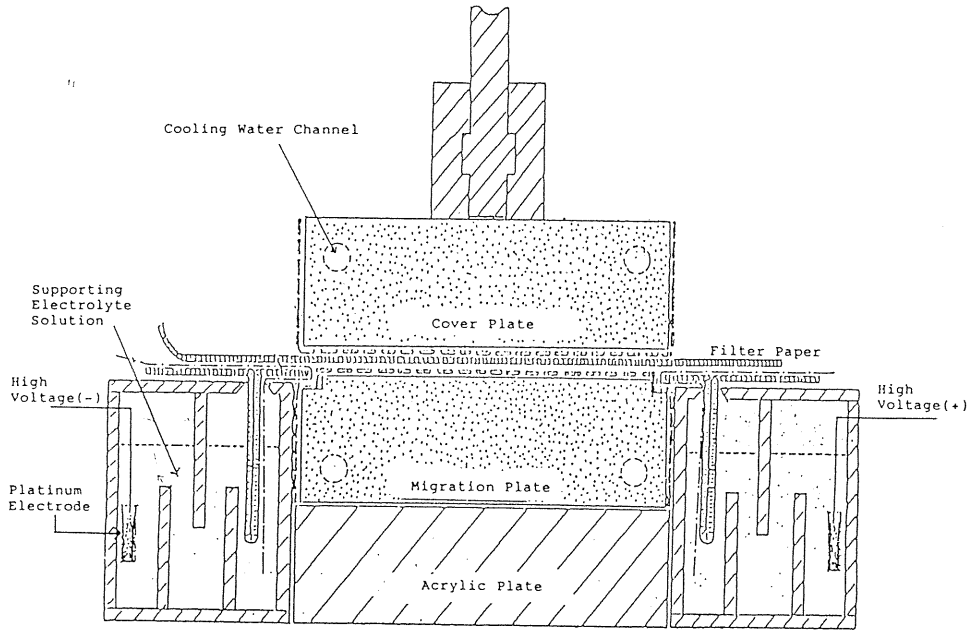

Fig. 22. Migration apparatus for the paper electrophoresis.

10^{-2} M uranyl nitrate embodying ^{235}U enriched to about 93% in mass 235 was irradiated under a thermal neutron flux of 1.5×10^{12} n/cm^{2}s at the TRIGA-II reactor. Chemical separation procedures, rapid paper electrophoresis[44,45], was made to separate the element of interest from fission products. An apparatus for this method is shown in Fig. 22. The supporting electrolyte solution was prepared by dissolving nitrilotriacetic acid (NIA) in a mixture of HCl to produce concentration of 4×10^{-3} M (pH = 1.8). The irradiated ^{235}U samples were dropped on the filter paper, and a high voltage electric potential was applied for a short time (depending on the element to be studied) for migration of elements. Separated nuclides were sealed in a polyethylene tubes and sent by a pneumatic system to a counting room. Beta-ray and gamma-ray spectra were measured by a Ge(Li), a NaI(Tl) and a plastic detectors in singles and coincidence modes.

Decay of ^{144}La: Cerium 144, with 86 neutrons is a transitional nucleus situated midway between the 82 neutron closed shell and deformed region that sets in at 90 neutrons. The spectroscopic study of the radioactive decay of ^{144}La is only one method for the study of the level properties of this neutron rich even-even nucleus ^{144}Ce. Until several years ago, there had been little information for the ^{144}La decay properties, since the sources of ^{144}La could not be produced by the ordinary nuclear reaction process except the fission process, and the separation of rare earth elements were rather difficult. Recently, various methods to obtain radioactive elements of rare earth region have been developed. Among them, the paper electrophoretic method developed by Ohyoshi *et al*[44] and Tamai *et al*[45] was applied for the present experiment[46]. The sources were prepared from the fission products of ^{235}U with above mentioned method. After the migration of radioactive source on the paper, where an electric potential of 5 kV/10 cm was applied for 20 s, the zone of lanthanum was cut, sealed

in a small polyethylene tube and transported to the counting room. An over-all time from the end of the irradiation until the start of counting was about 40 s. Beta- and gamma-ray spectra were measured. The half-life of ^{144}La was 40.6 ± 1.0 s. Total of 54 gamma-rays, including 17 new ones were observed and 46 of them are incorporated in a proposed decay scheme which includes 11 new levels. The Fermi-Kurie plot analysis of observed beta-spectra gave an end point energy of the highest beta component as 3.5 ± 0.2 MeV. The gamma-beta coincidence spectra gave beta-ray components with the end point energies of 3.37 ± 0.10, 2.80 ± 0.15, 2.83 ± 0.10 and 3.06 ± 0.10 MeV as shown in Fig. 23. From these results, it can be said that

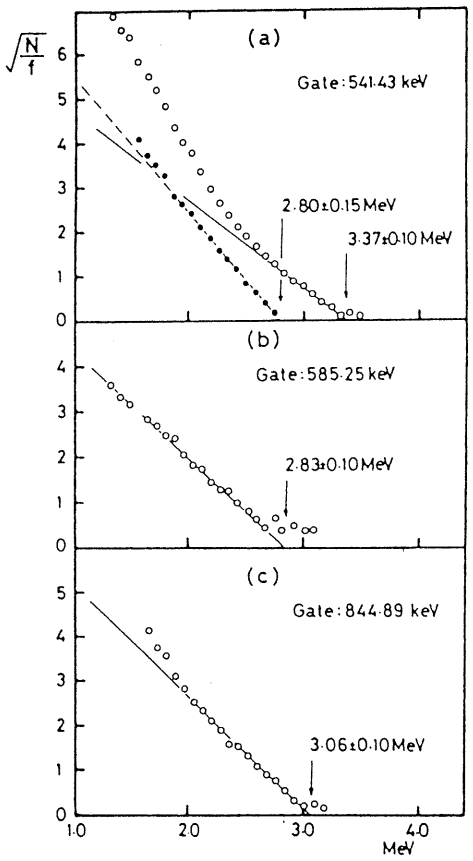

Fig. 23. Fermi-Kurie plots of β-ray spectra in coincidence with the 541.43, 585.25 and 844.89 keV γ-ray peaks.

no direct beta transition to the ground and first excited state of ^{144}Ce. The Q_β value of the decay was deduced as 4.3 ± 0.1 MeV. A decay scheme of ^{144}La was proposed as shown in Fig. 24. Characters of levels were still not yet clear and precise discussion on this nuclide is not possible at present. However, in comparison with other N = 86 transitional nuclei, the quasi band description[33] would be a reasonable model. The decay data itself are also important for the evaluation of the decay heat of reactor power.

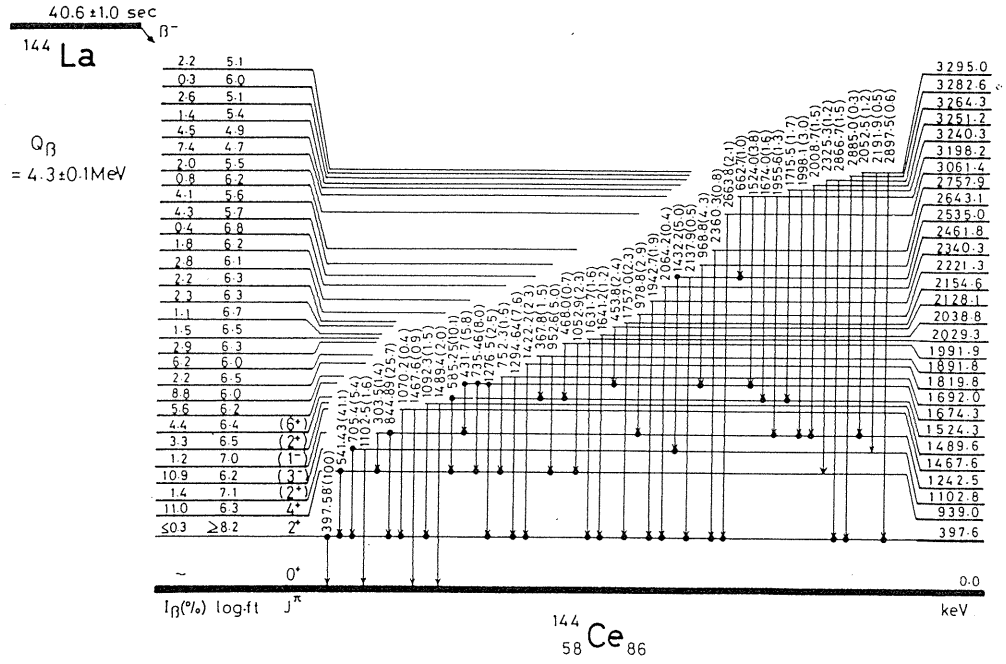

Fig. 24. A proposed decay scheme of 40.6 s ^{144}La.

Decay of ^{146}Pr: A study[47] to clarify the decay properties of ^{146}Pr was performed with the electrophoretic method. A Ge(Li), a pure Ge, a NaI(Tl) and a plastic detectors were used for the measurement of beta-rays and gamma-rays in singles and coincidence modes. Sources were prepared from fission products of ^{235}U by the paper electrophoresis. The electric potential of 3 kV/10 cm for migration was applied for 2 min. Over-all separation time was 3 min. The nuclei ^{146}Ce($T_{1/2}$ = 14 min), the parent nuclei of ^{146}Pr, was separated and then the ^{146}Pr was milked. A total of 104 gamma-transitions, 64 of them not reported before, have been observed and 88 transitions were incorporated into a decay scheme comprising 32 excited states of ^{146}Nd. Observed Q_β value was 4.15 ± 0.15 MeV. A proposed decay scheme is shown in Fig. 25. Gamma-gamma directional angular correlation measurements in ^{146}Nd have been performed to assign values of spin of excited states. The detectors used were a 50 cm^3 Ge(Li) detector fixed at a distance of 4.5 cm from the source. A 7.6 cmϕ × 7.6 cm NaI(Tl) detector was used for a movable detector at the distance of 9.6 cm from the source. The coincidence spectra were measured at the angles of 90°, 120°, 150° and 180° between the fixed and movable detectors. The coincidence window was set on the 453.9 keV transition from the 2^+ first excited state to the 0^+ ground state in ^{146}Nd. The observed full energy peaks of 12 cascade gamma-transitions with the 453.9 keV transition were analyzed with the following equation,

$$W(\theta) = 1 + A'_{22}P_2(\cos\theta) + A'_{44}P_4(\cos\theta) \quad (4)$$

where $A'_{kk} = (A_{kk}/A_{00})Q_{kk}$. The Q_{kk} are the geometrical correction factor for the NaI(Tl) and

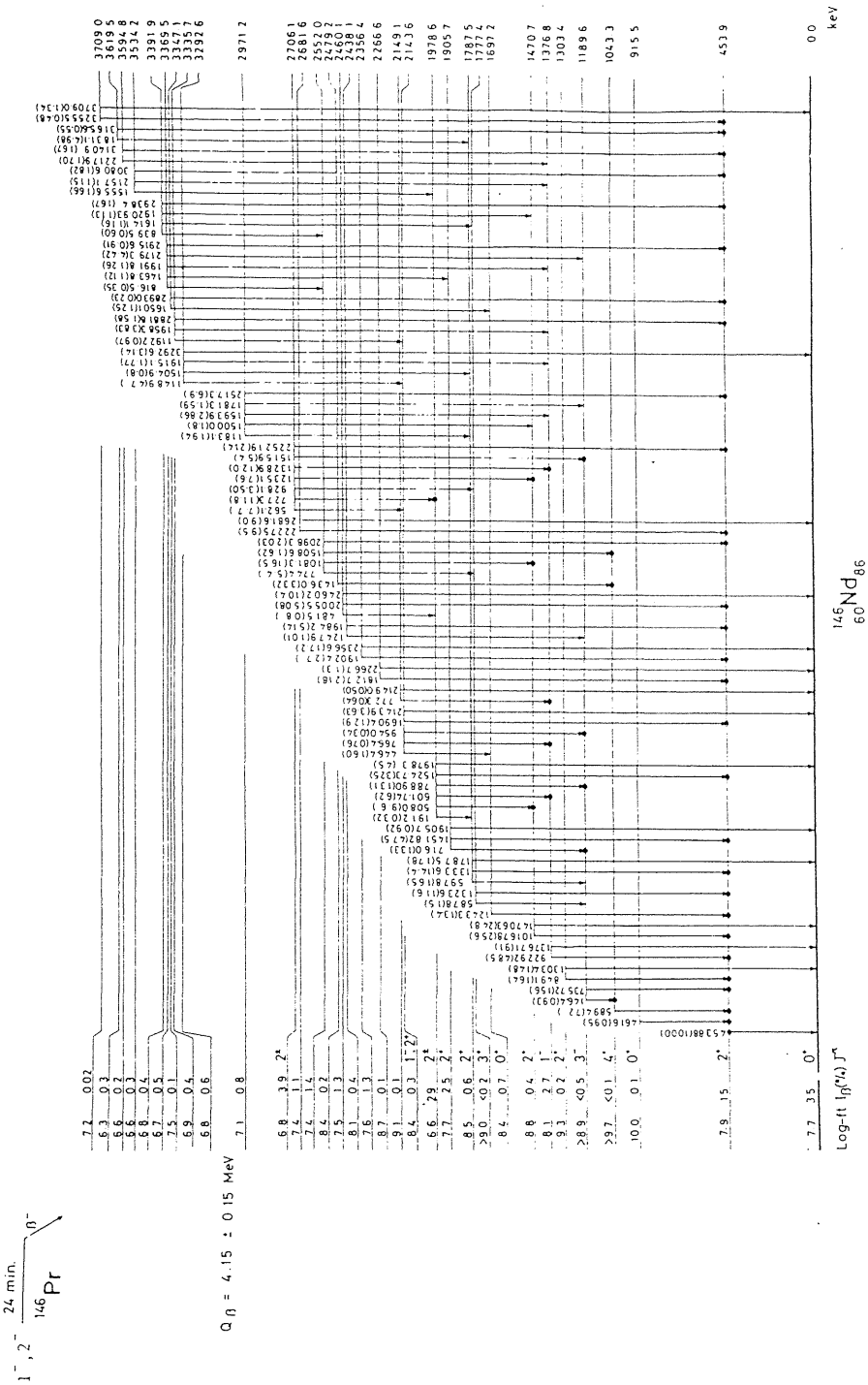

Fig. 25. A proposed decay scheme 24 min ^{146}Pr.

the Ge(Li) detector which were determined by the method of Krane[48]. The coefficients A_{22} and A_{44} determined spin sequences of three levels which concern the two transitions in cascade relation. Table 5. shows results of the angular correlation measurement, and probable spin sequence for each cascade is also shown in the Table 5. The quasi rotational pattern of levels has observed in many even-even nuclei[49]. Our study of ^{146}Pr presents confirmation of the quasi band structure. The pattern of levels in ^{146}Nd as shown in Fig. 25 is similar to that in ^{148}Sm[33] and ^{150}Gd[33] which have the same neutron number 86.

Table 5. Angular correlations in ^{146}Nd.

Cascade (keV)	A_2	A_4	Spin sequence	Mixing ratio δ	$L=2$(%)
589.4−453.9	0.01 ±0.17	0.09 ±0.31	1–2–0		
			2–2–0		
			3–2–0		
			4–2–0		
735.7−453.9	−0.015±0.017	0.006±0.031	*1–2–0		
			2–2–0		
			3–2–0	− 0.07± 0.02	<1.0
849.1−453.9	−0.23 ±0.46	0.09 ±0.90	2–2–0		
922.9−453.9	−0.255±0.044	−0.071±0.077	1–2–0	− 0.01± 0.04	<0.3
			*3–2–0		
1016.8−453.9	−0.133±0.074	0.399±0.142	2–2–0	$-12.5\ ^{+\ 7.6}_{-19.4}$	>99
1243.3−453.9	0.45 ±0.18	1.03 ±0.37	0–2–0		
1323.6−453.9	−0.36 ±0.15	0.14 ±0.30	1–2–0		
			2–2–0		
			3–2–0	$4.6\ ^{+60}_{-2.8}$	>80
1333.6−453.9	0.37 ±0.14	0.22 ±0.26	2–2–0	$1.44^{+\ 0.93}_{-\ 0.82}$	67^{+18}_{-39}
1451.8−453.9	0.463±0.053	0.099±0.099	2–2–0	$0.68^{+\ 0.56}_{-\ 0.42}$	32^{+29}_{-28}
1524.7−453.9	0.270±0.016	−0.029±0.029	2–2–0	0.03± 0.03	<0.4
			*3–2–0		
1690.4−453.9	−0.328±0.140	0.125±0.249	1–2–0	− 0.07± 0.13	<5
			2–2–0	− 2.5 ± 1.0	$86^{+\ 6}_{-17}$
			*3–2–0		
2252.2−453.9	0.411±0.103	−0.150±0.182	*1–2–0		
			2–2–0		

Mixing ratio δ was calculated from the value of A_2.
$L = 2$ (%) means the amount of quadrupole component in %.
*; Spin sequence is ruled out from the γ-ray decay pattern.

Decay of ^{143}La, ^{145}Ce, ^{146}Ce, ^{147}Ce, ^{147}Pr and ^{148}Pr: The decay of ^{143}La[50], ^{145}Ce[51], ^{146}Ce[51], ^{147}Ce[52], ^{147}Pr[50] and ^{148}Pr[53] were studied by using the paper electrophoresis. Beta-ray and gamma-ray spectra were measured by a Ge(Li), a NaI(Tl) and a plastic detectors in singles and coincidence modes.

A total of 76 gamma-rays including 23 new ones for ^{143}La, 32 gamma-rays including 14 new ones for ^{145}Ce, 26 gamma-rays including 6 new ones for ^{146}Ce, 14 gamma-rays including 4 new ones for ^{147}Ce, 86 gamma-rays including 9 new ones for ^{147}Pr and 40 gamma-rays including 4 new ones for ^{148}Pr were observed in our experiments. Observed Q_β values were 3.28 ± 0.10 for ^{143}La, 2.6 ± 0.1 for ^{145}Ce, 0.952 ± 0.05 for ^{146}Ce, 2.77 ± 0.10 for ^{147}Pr and

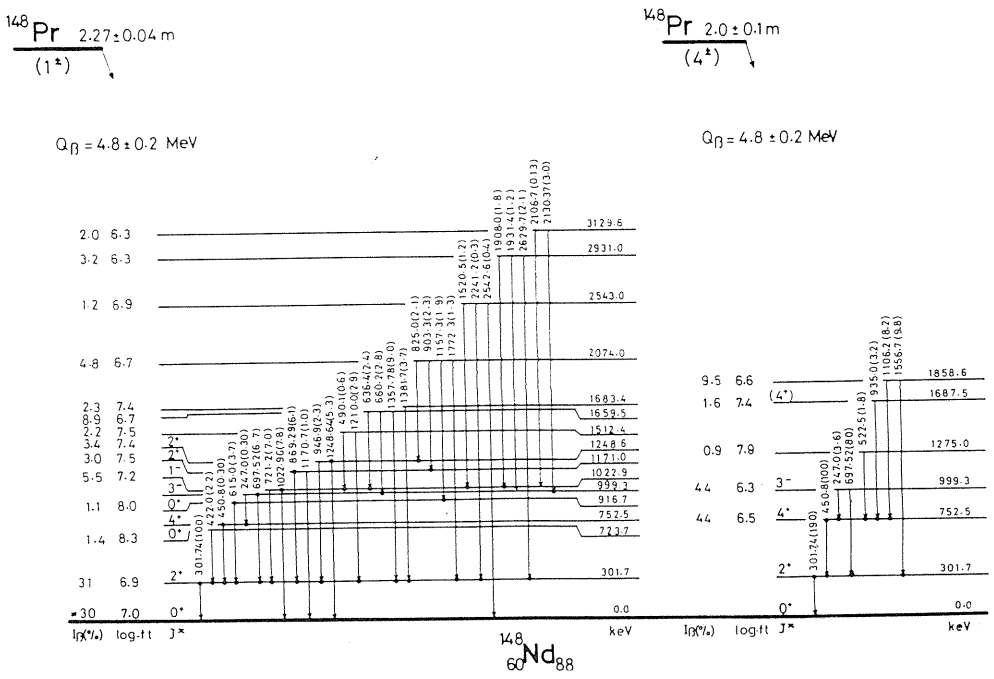

Fig. 26. A proposed decay scheme of 2.27 min ^{148}Pr.

4.8 ± 0.2 MeV for ^{148}Pr. The observed half-lives were 14.14 ± 0.16 min for ^{143}La, 3.01 ± 0.06 min for ^{145}Ce, 13.52 ± 0.13 min for ^{146}Ce, 57 ± 5 s for ^{147}Ce, 13.3 ± 0.4 min for ^{147}Pr and 2.27 ± 0.04 and 2.0 ± 0.1 min for close lying two isomers of ^{148}Pr.

A decay scheme was proposed for each nuclide. Five new levels were incorporated in the decay scheme of ^{143}La, 3 new levels in ^{145}Ce, one new level in ^{147}Ce, 4 new levels in ^{147}Pr and 6 new levels in ^{148}Pr. A decay scheme of ^{148}Pr proposed from our experiments is shown in Fig. 26. The decay scheme was revised from our previous report[32] (see Fig. 13). The decay scheme of ^{146}Ce was in good agreement with previous report[54], however, newly observed 12.23 keV gamma-ray confirmed existence of a level at 12.23 kev.

Deta obtained in our experiments are useful for the evaluation of decay heat power of nuclear reactor. Level structure of these nuclides were discussed in terms of the quasi band description[49].

4. 8 *Decay of Fission Products produced by Thermal Neutron Irradiation on ^{235}U and separated by the Liquid Chromatographic Method*

The decay of 11.6 min ^{152}Nd to levels of odd-odd ^{152}Pm has been studied[55] with HpGe, Ge(Li) detectors, LEPS and a plastic scintillation detector in gamma-ray singles, time dependent gamma-ray singles, gamma-gamma coincidence and beta-gamma coincidence modes. The sources were obtained from fission products of ^{235}U irradiated by the thermal neutrons. A rapid chemical separation procedure, the liquid chromatographic method, was applied for the separation of nuclide. A basic liquid chromatographic system was connected to an ion chromatograph with a single separation column containing a gel-type resin of

particle size of 10 μm. For the separation of rare earth ions from the solution of fission products, α-hydroxy isobutyric acid solution was used. The pH was adjusted to 4.6 with ammonium solution. The eluent were prepared with double distilled and deionized water. The eluent flow rate was 1.2 mℓ per minute. The irradiated uranyl nitrate was injected into the system. Eluent flowing out of the system was collected every 4 min and gamma-rays of each 4 min fraction were measured to confirm a separation pattern of rare earths in fission products. In each gamma-ray spectrum, intense gamma-ray peak counts were followed. Neodymium was separated from fission products within about 10 min. The radioactivity were collected in liquid. Liquid sources were precipitated using an oxalic acid and filtered in filter paper. The size of the source was 10 mm in diameter. The gamma-ray singles spectra were measured with a HpGe, a Ge(Li) and a planer(LEPS) detectors. The gamma-gamma coincidence measurements were performed in two parameter mode with the HpGe, Ge(Li) and a LEPS detectors. The beta-gamma delayed coincidence measurements were performed with the LEPS combined with a plastic scintillation counter. The half-life of ^{152}Nd was measured by following the gamma-rays in a spectrum multi-scaling mode. Ten gamma-rays were observed and five of them were new ones. The absolute intensity of the 278.5 keV gamma-ray per 100 decays was estimated by using the gamma-ray in ^{151}Nd, which was in the neodymium fraction and seen in the spectrum. The absolute intensity of the 278.5 keV gamma-ray was 0.29 $\pm$ 0.03. Internal conversion coefficients for the gamma-transition of 25.0 and 28.5 keV were determined from the coincidence spectrum gated by the 250.1 keV gamma-ray in the decay of ^{152}Nd (see Fig. 27). Analysis of the spectrum shows that the coefficient was 11.6 for the 28.5 keV transition and a probable multipolarity of this transition is M1 ($\leqq$ 6.0% E2), and the coefficient was 17.1 for the 25.0 keV transition and the multipolarity of this transition is probably M1 ($\leqq$ 8.2% E2).

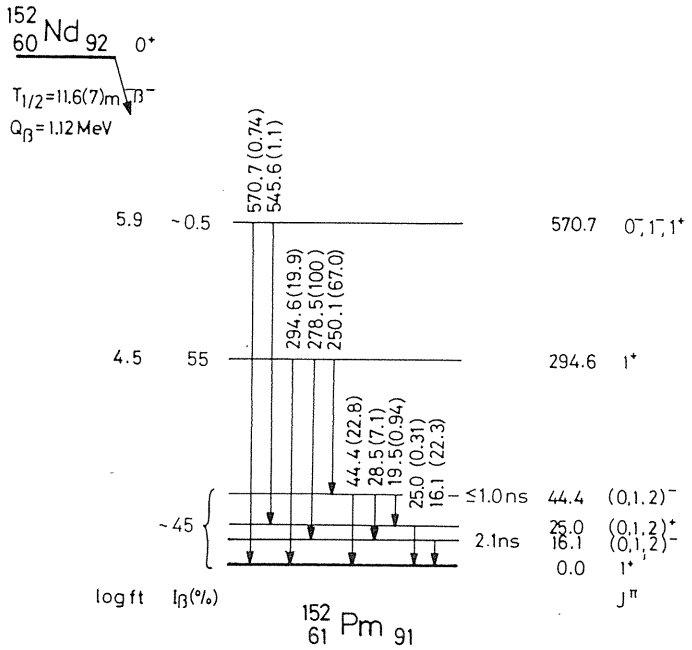

Fig. 27. A proposed decay scheme of 11.6 min ^{152}Nd.

The half-lives of the 16.1 and 28.5 keV gamma-ray emission were determined by means of a centroid shift method. The half-lives obtained were 2.1 ± 1.0 ns for the 16.1 keV transition and less than 1.0 ns for the 28.5 keV transition.

The half-life of the ^{152}Nd was measured in the spectrum multi-scaling mode, and deduced to be 11.6 ± 0.7 min. A proposed decay scheme is shown in Fig. 27, in which two new levels are shown at the energies of 25.0 and 570.7 keV. The Nilsson configurations of excited states in ^{152}Pm were discussed.

4. 9 Measurement of Short Half-lives by using an On-Line Isotope Separator

The nucleus ^{93}Sr is supposed to have a single particle character. Since the transition probability gives a sensitive information for the shell structure, the half-life and the multipolarity for the 213 keV transition in ^{93}Sr were measured[56]. The half-life for the 204 keV transition in ^{95}Sr was also determined. Radioactive elements of 5.9 s ^{93}Rb and 0.38 s ^{95}Rb were produced by the thermal neutron fission of ^{235}U and separated by a He jet type on-line isotope separator (KUR-ISOL)[4),5)] and by the gas filled recoil separator JOSEF at Forschungsanlage Julich, Germany[57]. The beta-gamma delayed coincidence technique was employed for the half-life measurement. The beta particles were detected by a plastic scintillator and gamma-rays by a Ge(Li) detector. The time signals from the time to amplitude converter and the energy signals of the detector were recorded on a magnetic tape in two parameter list mode. The mass separated Rb activities were collected on a transport tape and were periodically removed from the detector area to suppress long lived components. In Fig. 28, a time

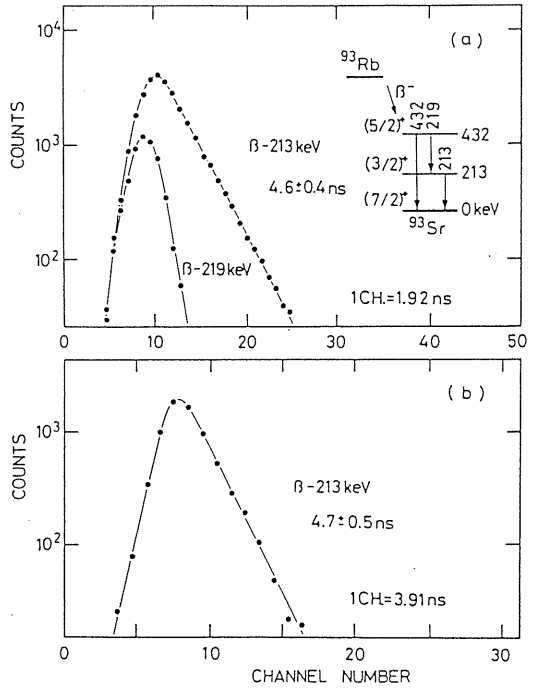

Fig. 28. (a) Time distribution obtained at KUR-ISOL for the β-213 keVγ in ^{93}Sr together with the prompt β-219 keVγ,
(b) Time distribution obtained at JOSEF, Julich, Germany.

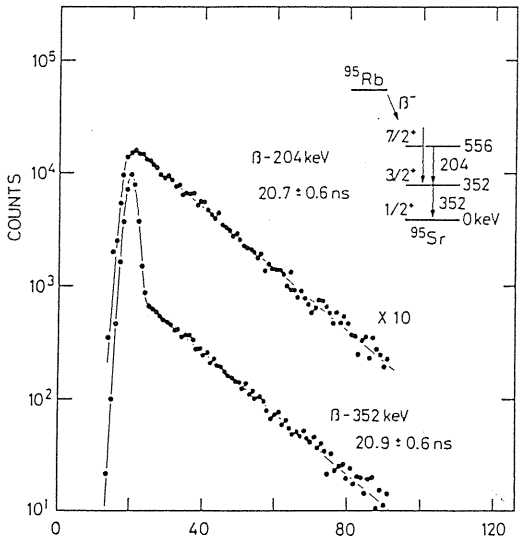

Fig. 29. Time distributions for the 204 keV and the 352 keV transitions in ^{95}Sr.

distribution obtained for the β-213 keV transition in ^{93}Rb is shown together with the one for the prompt 219 keV transition. The half-life was determined by applying the least square fits to the slope. An average value of the half-life measurements is 4.6 ± 0.3 ns. The centroid shift of the beta-213 keV gamma-ray curve corresponds to the mean life. The value obtained was in good agreement with the value obtained from the slope method. Fig. 29 shows time distributions for the 204 keV and 352 keV transitions in ^{95}Sr taken by KUR-ISOL. The time distribution of the 352 keV transition shows a prompt component in addition to a slope with a half-life of 20.9 ± 0.6 ns. The prompt one is due to the population of the 352 keV levels through gamma-rays other than the 204 keV one and from levels with shorter half-lives. The slope component is assigned to the half-life of the 556 keV level. An average value of the half-life was 20.8 ± 0.5 ns. The measurement at JOSEF gave the value of 21.3 ± 1.0 ns. The average of two measurements was 20.9 ± 0.5 ns for the 556 keV level. The X-γ coincidence measurements were performed to determine the internal conversion coefficient of the 213 keV transition. The observed K X-rays result from the internal conversion process of the 213 keV transition and then ratio of the intensities of the 213 keV gamma-ray and the X-ray considering the fluorescence yield gives a internal conversion coefficient. The value obtained for K conversion process was 0.056 ± 0.006 and assigned multipolarity was E2 ($\leqq$ 15% M1). The reduced transition probablities are deduced as B(E2) = (261^{+17}_{-43}) e^2fm^4 for 213 keV transition and (71 ± 2) e^2fm^4 for the 204 keV transition. These B(E2) values are comparable to the Weisskopf estimates and to those for the similar transitions in the neighbouring nuclei.

5. Measurement of Cross Sections of Nuclear Reaction by using Activation Method

The nuclear reaction cross sections have been measured by various methods. When the reaction products are radioactive elements, the total cross section can be obtained by measuring the activity of the products. The amount of activity is determined from the intensities of beta-rays and gamma-rays. Therefore, we applied the technique of measurement of gamma-ray and beta-ray to the cross section measurements.

5. 1 Measurement of Formation Cross Sections and Half-lives of Short-lived Nuclei produced by 14 MeV Neutrons

Neutron activation cross section data around 14 MeV have become important from the view point of fusion reactor technology, especially for evaluation of radiation damage, nuclear transmutation, induced activity and so on. Data of formation cross section of short-lived activities are scarce. A measuring program[58)-61)] for activation cross sections of short-lived nuclei by neutrons around 14 MeV has been carried out at the intense 14 MeV neutron source facility (OKTAVIAN) of Osaka University. Up to now, we have measured 64 cross sections for the (n, 2n), (n, p), (n, n'p) and (n, α) reactions leading to short lived nuclei in a qualified experimental condition.

The activation cross section values were obtained by measuring radioactivities induced with neutron irradiation as follows:

$$C = N\sigma\phi\varepsilon_f I_r [1-exp(-\lambda t_i)] [exp(-\lambda t_c)] [1-exp(-\lambda t_m)]/\lambda \tag{5}$$

where
- C: gamma-ray peak count,
- N: number of target nuclei,
- σ: activation cross section to be measured,
- ϕ: neutron flux at the irradiation position,
- ε_f: full energy peak detection efficiency of gamma-ray,
- I_r: gamma-ray emission probability per disintegration,
- λ: decay constant of induced radioactivity,
- t_i: irradiation time,
- t_c: cooling time,
- t_m: measuring time of gamma-ray.

All cross section values were obtained relative to the standard cross section of reaction $^{27}Al(n,\alpha)^{24}Na$[62)]. Samples were set around a rotating T-target as shown in Fig. 30. The angle of irradiation positions to the direction of d^+ beam were 0°, 50°, 75°, 105° and 155°, which covered the neutron energies ranging from 14.9 to 13.4 MeV. The effective energy of incident neutrons at each irradiation position was determined by the ratio of the $^{90}Zr(n,2n)^{89}Zr$[63)] and $^{93}Nb(n,2n)^{92m}Nb$[64)] cross sections (Zr/Nb method[65)]). Another pneumatic tube was set at −105° to check the accuracy of angle. The distance between the T-target and the irradiation position was 15 cm. When high neutron flux was required, an additional tube set at 0° and at a distance of 1.5 cm was used as shown in Fig. 30. Since half-lives of most of induced activity in our experiments were short lives, the neutron flux at the sample position was measured with use of substandard reaction $^{27}Al(n,p)^{27}Mg$ ($T_{1/2} = 9.46$ min), whose cross section were determined by referring to the standard reaction $^{27}Al(n,\alpha)^{24}Na$[62)]. The samples were sandwiched between two aluminum foils of 10 mm × 10 mm × 0.2 mm thick. The use of substandard reaction $^{27}Al(n,p)^{27}Mg$ brought only an additional uncertainty of 0.5% to final results.

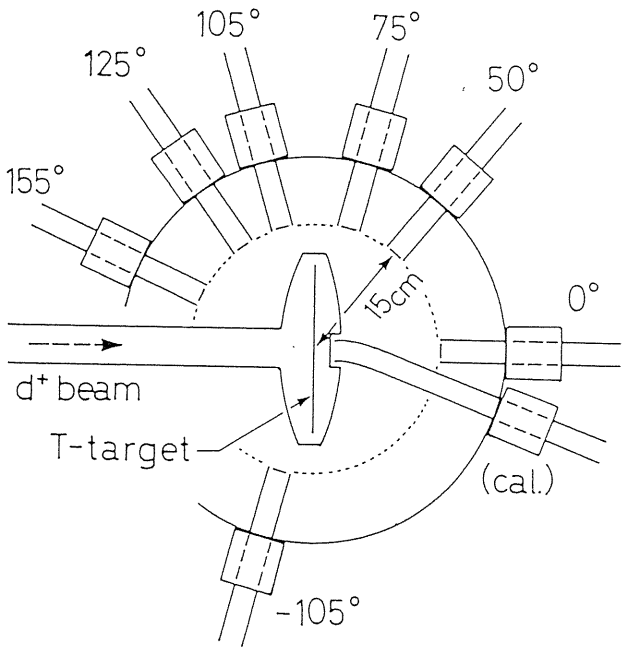

Fig. 30. A pneumatic sample transport system at OKTAVIAN.

Irradiated samples were transported through a pneumatic tube system to the counting room. Gamma-rays emitted from the irradiated samples and the monitor aluminum foils were measured with 12% and 4% HPGe detectors and a 16% HPGe detector, respectively. Foils of Nb and Zr for neutron energy determination were measured with a 22% HPGe detector. Each detector was covered with a 5 mm thick acrylic absorber in order to reduce beta-rays. The peak efficiency calibration at 5 cm was accomplished by using gamma-ray sources of ^{24}Na, ^{56}Co, ^{133}Ba, ^{152}Eu and ^{154}Eu. Corrections for true coincidence sums were applied. The errors in the efficiency curves were estimated to be 1.5% for energies above 300 keV, 3% between 300 and 80 keV, and 5% below 80 keV. To measure the weak activities efficiently, the sampls were put on the absorber surface (source-to-detector distance is 5 mm). Calibration measurements were carried out to convert the efficiency at 5 mm to the one at 5 cm at both distance by using extra samples irradiated with rather strong neutron flux through the pneumatic tube set at 1.5 cm. This method improved the detection efficiency by a factor of about 7. This calibration procedure brought an additional error of 1.0% to the results. The following principal corrections in deducing cross sections were performed:

1) fluctuation of the neutron flux during the irradiation,
2) contribution of scattered low energy neutrons,
3) true coincidence sum,
4) random coincidence sum,
5) deviation in measuring position coming from different thickness of each sample,
6) self-absorption of the gamma-ray in the sample,
7) interfering reaction producing activities emitting the gamma-ray with the same energy of interest,

The details of procedures are described elsewhere[58),59)].

The total errors (δ_t) were derived by combining the experimental error (δ_e) and the error (δ_r) of nuclear data in quadratic: $\delta_t^2 = \delta_e^2 + \delta_r^2$. Estimated major error sources are listed in Table 6. When good counting statistics were achieved, the experimental and total errors were 2.4% and 6.0%, respectively. The main error sources were due to the gamma-ray detection efficiency and standard $^{27}Al(n,\alpha)^{24}Na$ reaction cross section. In some cases, the error of the gamma-ray emission probability were dominant. When the error of nuclear data is reduced, the total error will be much improved.

Table 6. Principal sources of uncertainly in the measured cross sections.

Experimental error (δ_e)	
Source of error	Uncertainty(%)
Counting statistics	0.5 - 29
Sample mass including purity	0.1
Neutron flux fluctuation	< 0.1 (20% of correction)
Gamma-peak area evaluation	0.5
Detector efficiency	1.5 (Eγ > 300keV)
	3 (300-80 keV)
	5 (Eγ < 80 keV)
Efficiency calibration at 0.5 and 5 cm	2.0
Correction for	
true coincidence sum	< 17
random coincidence sum	< 0.4
sample thickness	0.6-1.4 (20% of correction)
self-absorption of γ-rays	0-2.6 (20% of correction)
low energy neutrons	0.7 (30-40% of correction)
Secondary reference cross section for $^{27}Al(n,p)^{27}Mg$	0.5(Only statistics)

Error of nuclear data(δ_r)	
Source of error	Uncertainty(%)
Reference cross section $^{27}Al(n,\alpha)^{24}Na$ (ENDF/B-V)	3.0
Absolute γ-ray intensity	0-20
Half-life	0-5

Table 7. Reactions of cross section measurement.

Reaction	$T_{1/2}$	Reaction	$T_{1/2}$
$^{14}N(n,2n)^{13}N$	9.96 m	$^{71}Ga(n,\alpha)^{68m}Cu$	3.75 m
$^{19}F(n,p)^{19}O$	26.91 s	$^{87}Rb(n,2n)^{86m}Rb$	1.017m
$^{25}Mg(n,p)^{25}Na$	59.6 s	$^{87}Rb(n,\alpha)^{84m}Br$	6.0 m
$^{26}Mg(n,\alpha)^{23}Ne$	37.6 s	$^{86}Sr(n,p)^{86m}Rb$	1.017m
$^{26}Mg(n,np)^{25}Na$	59.6 s	$^{87}Sr(n,np)^{86m}Rb$	1.017m
$^{28}Si(n,p)^{28}Al$	2.241m	$^{88}Sr(n,p)^{88}Rb$	17.8 m
$^{29}Si(n,p)^{29}Al$	6.56 m	$^{89}Y(n,\alpha)^{86m}Rb$	1.017m
$^{29}Si(n,np)^{28}Al$	2.241m	$^{94}Zr(n,p)^{94}Y$	18.7 m
$^{30}Si(n,\alpha)^{27}Mg$	9.46 m	$^{92}Mo(n,2n)^{91g}Mo$	15.48 m
$^{30}Si(n,np)^{29}Mg$	6.56 m	$^{97}Mo(n,p)^{97m}Nb$	1.0 m
$^{31}P(n,2n)^{30}P$	2.50 m	$^{98}No(n,n'p)^{97m}Nb$	1.0 m
$^{31}P(n,\alpha)^{28}Al$	2.241m	$^{101}Ru(n,p)^{101}Tc$	14.2 m
$^{32}S(n,t)^{30}P$	2.50 m	$^{102}Ru(n,p)^{102m}Tc$	4.35 m
$^{37}Cl(n,p)^{37}P$	5.05 m	$^{102}Ru(n,np)^{101}Tc$	14.2 m
$^{50}Ti(n,p)^{50m,g}Sc$	1.710m	$^{104}Ru(n,p)^{104}Tc$	18.3 m
$^{51}V(n,p)^{51}Ti$	5.76 m	$^{104}Ru(n,\alpha)^{101}Mo$	14.6 m
$^{52}Cr(n,p)^{52}V$	3.75 m	$^{104}Pd(n,p)^{104m}Rh$	4.34 m
$^{53}Cr(n,p)^{53}V$	1.61 m	$^{105}Pd(n,p)^{105m}Rh$	42.4 s
$^{53}Cr(n,np)^{52}V$	3.75 m	$^{105}Pd(n,np)^{104m}Rh$	4.34 m
$^{54}Cr(n,p)^{54}V$	49.8 s	$^{106}Pd(n,np)^{105m}Rh$	42.4 s
$^{54}Cr(n,np)^{53}V$	1.61 m	$^{108}Pd(n,2n)^{107m}Pd$	21.3 s
$^{54}Cr(n,p)^{51}Ti$	5.76 m	$^{108}Pd(n,p)^{108g}Rh$	6.0 m
$^{54}Fe(n,2n)^{53g}Fe$	8.51 m	$^{108}Pd(n,np)^{107}Rh$	21.7 m
$^{60}Ni(n,p)^{60m}Co$	10.47 m	$^{107}Ag(n,p)^{107m}Pd$	21.3 s
$^{62}Ni(n,p)^{62m}Co$	13.91 m	$^{112}Cd(n,\alpha)^{109m}Pd$	4.69 m
$^{62}Ni(n,p)^{62g}Co$	1.50 m	$^{113}In(n,2n)^{112m}In$	20.9 m
$^{64}Ni(n,\alpha)^{61}Fe$	5.98 m	$^{113}In(n,2n)^{112g}In$	14.4 m
$^{63}Cu(n,\alpha)^{60m}Co$	10.47 m	$^{116}Cd(n,p)^{116g}Ag$	2.68 m
$^{66}Zn(n,p)^{66}Cu$	5.10 m	$^{119}Sn(n,p)^{119g}In$	2.4 m
$^{67}Zn(n,np)^{66}Cu$	5.10 m	$^{119}Sn(n,p)^{119m}In$	18.0 m
$^{68}Zn(n,p)^{68m}Cu$	3.75 m	$^{120}Sn(n,p)^{120m}In$	43.5 s
$^{69}Ga(n,\alpha)^{66}Cu$	5.10 m	$^{120}Sn(n,p)^{120m'}In$	45.6 s

The reactions, of which cross sections were measured in this study, are listed in Table 7, and the results of the measurements are shown elsewhere[58)-61)]. Some data were obtained for the first time. Examples of cross section curves around 14 MeV are shown in Fig. 31 to 34. In Figs. 31 and 32, the cross sections of reactions $^{102}Ru(n, np)^{101}Tc$ and $^{105}Pd(n,np)^{104m}Rh$ are shown, respectively. No previous cross section data are seen for these reactions and it might be due to too small values (less than 5 mb). In Figs. 33 and 34, cross sections of reactions $^{101}Ru(n,p)^{101}Tc$ and $^{108}Pd(n,np)^{107}Rh$ are shown. The values of cross sections are different from the previous data by factor of more than 10 for ^{101}Ru[66)] and more than 2 for ^{108}Pd[67)].

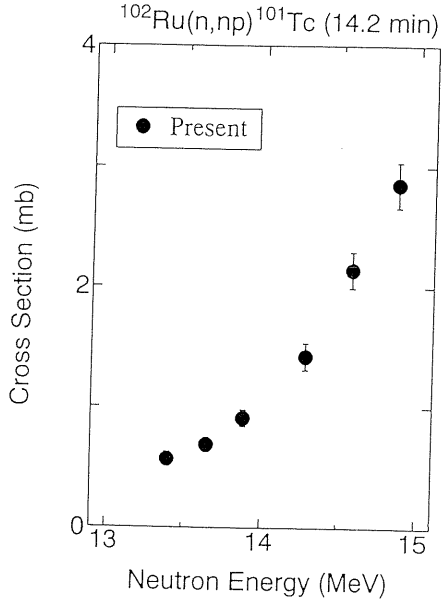

Fig. 31. Cross sections of ^{102}Ru(n,np)^{101}Tc reaction.

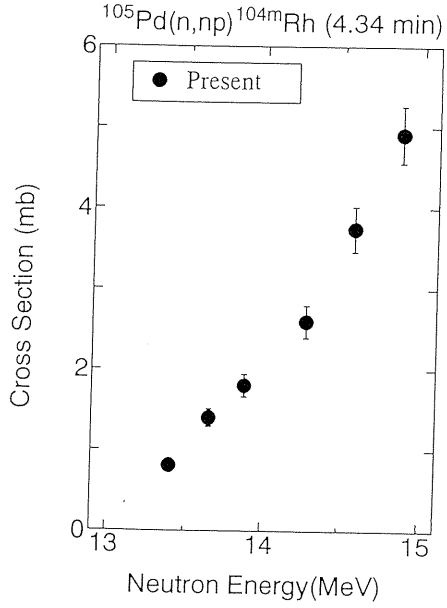

Fig. 32. Cross sections of ^{105}Pd(n,np)^{104m}Rh reaction.

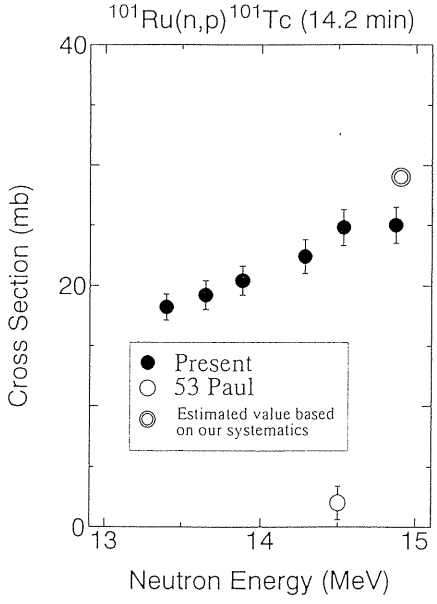

Fig. 33. Cross sections of ^{101}Ru(n,p)^{101}Tc reaction.

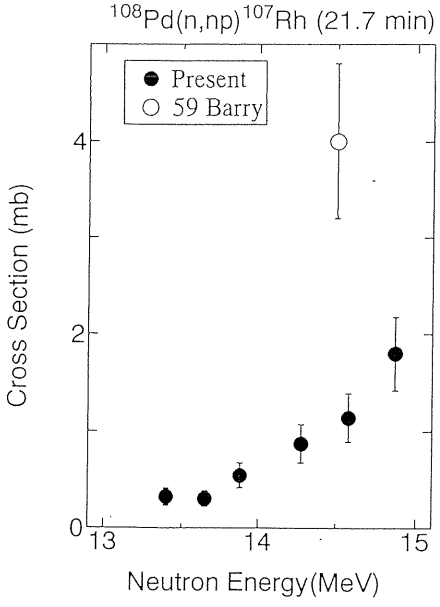

Fig. 34. Cross sections of ^{108}Pd(n,np)^{107}Rh reaction.

In Fig. 33, an estimated values based on the systematics[68] is shown. The systematics is expressed by the following formula:

$$\sigma_{np}(mb) = (6.0 \times 10^{-4})A^{5.7}(0.585)^{b}exp[-33(N-Z)/A + \delta], \quad (6)$$

$$b = (\ln A)^2,$$

$$\delta = \begin{cases} 0 \text{ for even-even target nucleus} \\ +0.15 \text{ for even-odd nucleus} \\ -0.15 \text{ for odd-even nucleus} \end{cases}$$

where N, Z and A are neutron, proton and the mass number of the target nucleus, respectively. The present estimated value is close to our experimental value.

The half-life values are one of the important decay data. Especially, the precise and reliable half-life data are necessary to obtain the values of cross section from the measured intensities of gamma-rays. We measured[59)-61)] the half-lives of activities produced by the fast neutron irradiation. The gamma-rays were measured with the Ge detector in the spectrum multi-scaling mode. The measurements were made at equal intervals of 1/3 to 1/6 of the half-life for about 10 times of the half-life. The sources of ^{137}Cs, ^{170}Tm and ^{241}Am and a pulse generator with a rate of 60 cps were simultaneously measured together with the short-lived activity for the correction of the pile-up and the dead time losses (source method, constant-pulser method). The initial counting rates were always kept to be less than 9×10^3 cps. Data points were analyzed by the least square fitting. The detail of procedures are described in elsewhere[69]. It was found that the corrections of the pile-up and the dead time losses were insufficient for the previous data and the values reported previously were rather long. Results of our cross section measurements are shown in Refs. 58–61.

5. 2 *Measurement of Formation Cross Sections of Long-lived (with Half-lives over 1 min) Nuclei*

Formation cross sections of long-lived (half-life: more than 1 min) nuclei by using 14 MeV neutrons were measured[70] systematically for the energy range from 13.3 to 15.0 MeV at the Intense Fast Neutron Source Facility (FNS) of Japan Atomic Energy Research Institute (JAERI). Up to now, 110 cross section data for reactions of (n, p), (n, np'), (n, α) and (n, 2n) in 26 elements including major structural materials of a fusion reactor, such as iron, nickel, chromium, titanium, molybdenum, etc. were measured in a unified experimental condition. To carry out such many measurements in a short time an efficient gamma-ray measuring method was introduced by employing multiple detectors. The all data measured were carefully examined. The incident neutron energies were determined by using a Monte Carlo calculation. Experimental errors were within $\pm 5\%$ for almost all data. The present data showed signifificant improvement in accuracy in comparison with previously reported data. Measured data are presented in Ref. 70.

5. 3 *Measurement of Reaction Cross Section by using an On-Line Isotope Separator*

The reaction cross section of ^{63}Cu(p,3n)^{61}Zn was measured[71] by using an on-line isotope separator (ISOL) at proton energies from 30 to 52 MeV. We attempted to determine the cross section of the short-lived ^{61}Zn($T_{1/2} = 1.48$ m) isotope with ISOL attached to the frequency-modulation (FM) cyclotron at the Institute for Nuclear Study, University of Tokyo.

The ISOL consists of a target-ion source, an analyzing magnet, collector chamber and a moving tape chamber. Details of the performance of the ISOL has been reported elsewhere[72]. Delay time between the production of activity at the target-ion source and measurement was 1 min by using an improved target-ion source. A natural copper foil of 10 μm thickness was used as a target. This target was bombarded by proton beam of the cyclotron. The proton energy was degraded with aluminum foils in front of a target-ion source part. The zinc radioisotopes produced by proton bombardment were evaporated from the target heated up to 1000°C, and were rapidly ionized. Extracted ions were separated with the analyzing magnet and focused in a collector chamber. One of the separated beams selected with a slit in the collector chamber was passed through a shielding wall and transported to the tape chamber. Collected radioactivity on a movable tape was measured with GM counters at two positions of windows of the tape chamber. The delay time was measured by using ^{63}Zn ($T_{1/2} = 38.6$ m) and was 0.9 ± 0.1 min. The cross section ratio was obtained from the ratio of integrated counts of the ^{61}Zn and ^{63}Zn in mass spectra. The radioactive Zn isotopes were measured with a GM counter at the tape chamber by sweeping the magnet field. After 1 min collection of the isotopes on the tape, the tape was moved and the collected isotopes were transferred by the tape to the measuring point. The radioisotopes of ^{61}Zn was well separated from ^{63}Zn. The fluctuation of the beam current of the protons was within 10%. In order to monitor the ion beam, one of the ion currents of the stable isotopes ^{63}Cu and ^{61}Cu was measured with a pole set in the collector chamber. The cross sections were also measured by the stacked foil method and both results were consistent as shown in Fig. 35. The maximum value of the cross section was 6.2 ± 0.7 mb at the proton energy of 39 MeV.

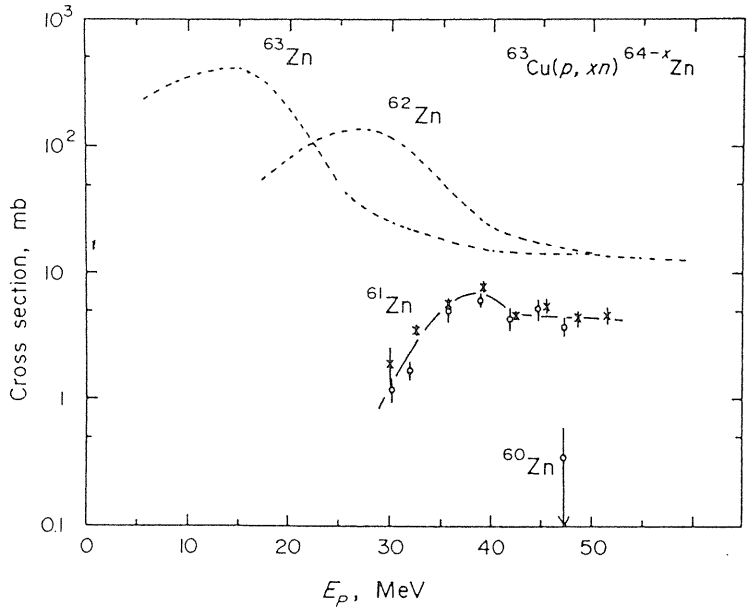

Fig. 35. Cross section of ^{63}Cu(p,3n)^{61}Zn reaction, Open circles were obtained by the ISOL experiment, crosses were given by the stacked foil method. The broken curves indicate the excitation functions of ^{63}Cu(p,n)^{63}Zn and ^{63}Cu(p,2n)^{62}Zn reactions.

5. 4 *Measurement of Activation Cross Sections by using Fast Neutron from the 2 MeV Van de Graaff*

The 2 MeV Van de Graaff accelerator of Nagoya University was used[73)-75)] for the measurement of activation cross section. The fast pneumatic tube system[3)] was employed for the transfer of the activated samples. The activities were measured by a Ge(Li) detector. The cross section for the formation of the ^{207}Pb for neutron energies from 4.1 to 5.2 MeV have been measured[73)]. The experimentally determined value of the cross section increased from 316 ± 44 mb to 788 ± 110 mb with increase of energy of above mentioned energy region. The cross sections for the reactions ^{90}Zr(n,n')^{90m}Zr, ^{91}Zr(n,2n)^{90m}Zr, ^{207}Pb(n,n')^{207m}Pb and ^{208}Pb(n,2n)^{207m}Pb for neutron energy of 14.8 MeV have been measured by means of the activation method[74)]. The cross sections were determined with reference to the known ^{27}Al(n,α)^{24}Na reaction cross section. Enriched isotopes, ^{90}Zr, ^{91}Zr, ^{207}Pb and ^{208}Pb were used as targets. The irradiation and the activity measurements were repeated 100 times to obtain good statistics. The cross sections obtained are 410 ± 40 mb for ^{90}Zr(n,n')^{90m}Zr, 775 ± 65 mb for ^{91}Zr(n,2n)^{90m}Zr, 160 ± 23 mb for ^{207}Pb(n,n')^{207m}Pb, 1220 ± 100 mb for ^{208}Pb(n,2n)^{207m}Pb. From this results, the effective formation cross sectios of ^{90m}Zr and ^{207m}Pb for natural Zr and Pb have been estimated as 475 ± 40 mb and 900 ± 80 mb, respectively. The neutron activation cross section of 16 reactions on Mo isotopes have been measured for 14.8 MeV neutron[75)]. The cross sections have been determined with reference to the known ^{27}Al(n,α)^{24}Na and the ^{27}Al(n,p)^{27}Mg reaction. The cyclic activation and measurement sequence[3)] was employed for the measurement of short-lived activities. Measured reactions were (n,2n), (n,p) and (n,α) reactions on the Mo isotopes. The cross sections of ^{98}Mo(n,np)^{97m}Nb and ^{98}Mo(n,np)^{97g}Nb reactions were also determined. Results are reported in Ref. 75. The exponential dependence on (N−Z)/A of the (n,p) reaction cross sections are discussed.

6. Measurement of Neutron Cross Sections of Long-lived Fission Products

As one of methods of the management of radioactive nuclear waste, the nuclear transmutation of the waste nuclides has been investigated. Feasibility of the use of high flux fission reactor and high intensity accelerators has been studied as intense neutron sources for the transmutation. It is necessary to obtain neutron cross sections for the investigation because the cross sections determine the transmutation rate. The ^{137}Cs ($T_{1/2}$ = 30 y) and ^{90}Sr ($T_{1/2}$ = 28 y) are important nuclides for the waste management. Values of neutron cross sections of these nuclides were inaccurate because they are radioactive and then handling of them as target is difficult and radiations from original elements becomes background of the gamma-ray measurement. We performed measurements of neutron capture cross sections of these nuclides[76)-78)] by the activation method by a new idea, and chemical separation technique were also used to reduce impurity activities.

6. 1 *Measurement of Thermal Neutron Cross Section and Resonance Integral of the Reaction ^{137}Cs(n,γ)^{138}Cs*

The thermal neutron cross section and the resonance integral of the ^{137}Cs(n,γ)^{138}Cs ($T_{1/2}$ = 32 m) reaction have been measured[76),77)] by means of a modified Cd-ratio technique. Targets of about 0.4 MBq of ^{137}Cs were irradiated with neutrons in the JRR-4 swimming pool type reactor at Japan Atomic Energy Research Institute (JAERI) by using a pneumatic tube equipment with a movable Cd shield. The irradiations were carried out without the Cd

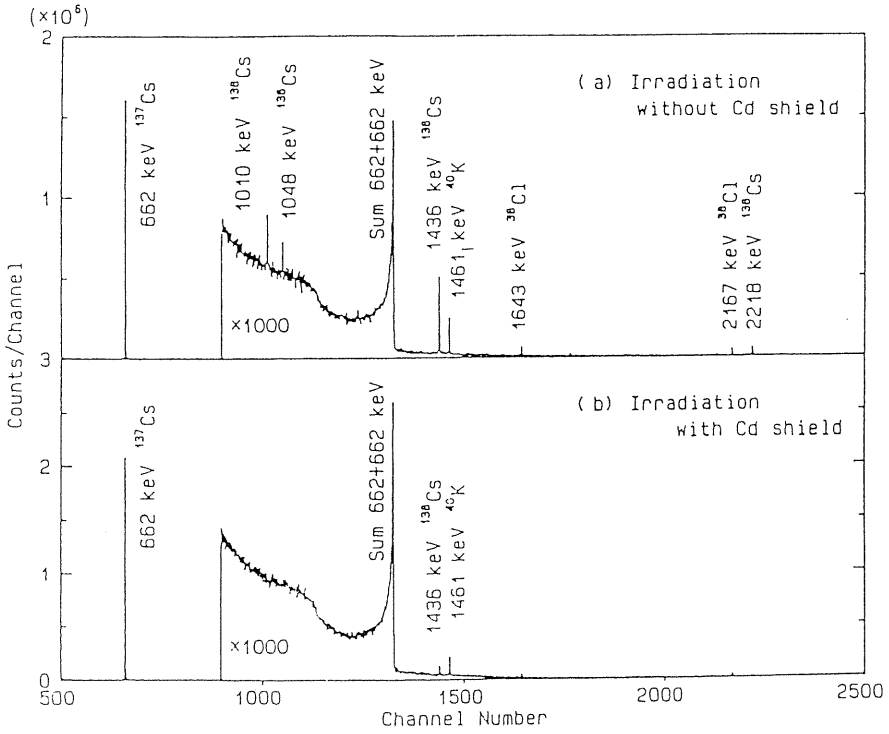

Fig. 36. Gamma-ray spectra of ^{137}Cs samples irradiated by thermal neutrons (a) without a Cd shield, and (b) with a Cd shield, and purified.

shield and with the Cd shield. The neutron fluxes and its epithermal fractions were monitored with activation detectors (Co/Al and Au/Al) whose sensitivity to epithermal neutrons differed from each other. After the irradiation, the irradiated ^{137}Cs samples were purified chemically and their gamma-ray spectra were measured with a high purity Ge detector with a large efficiency. The cross section and the resonance integral were obtained by comparing the gamma-ray intensity seen in the spectra (see Fig. 36). The radioactivity $\lambda_2 N_2$ of a nuclide with the decay constant λ_2, produced with a rate R during an irradiation period t, is given by

$$\lambda_2 N_2 = N_1 R[1 - exp(-\lambda_2 t)] \tag{7}$$

where N_1 is the number of the target nuclei, variation of N_1 during the irradiation is assumed to be negligible.

For a radioactive target nuclide with the decay constant λ_1, Eq. (7) is rewritten as

$$\frac{\lambda_2 N_2}{\lambda_1 N_1} = \frac{R}{\lambda_1}[1 - exp(-\lambda_2 t)] \tag{8}$$

for gamma-ray emitters of the target and product nuclides; the activity ratio $\lambda_2 N_2/\lambda_1 N_1$ can

be obtained from an observed gamma-ray spectrum. Using Eq. (8), the value of R can be deduced from the measured activity ratio. When an effective cross sectio $\hat{\sigma}$ for well moderated neutrons is expressed by the Westcott convention[79], R is given by

$$R = nv_0\hat{\sigma} \tag{9}$$

where nv_0 is the "neutron flux" in the Westcott convention with the neutron density n, including thermal and epithermal neutron, and with the neutron velocity $v_o = 2{,}200$ m/s and

$$\hat{\sigma} = \sigma_0[gG_{th} + r(T/T_0)^{1/2}s_0 G_{epi}] \tag{10}$$

Here, σ_0 is the reaction cross section for 2,200 m/s neutrons, and g the measure of the cross section deviation from the 1/v law in the thermal energy region. The quantity $r(T/T_0)^{1/2}$ gives the fraction of epithermal neutrons in the neutron spectrum and s_0 is defined by

$$s_0 = (2\pi^{-1/2})\,(I'_0/\sigma_0) \tag{11}$$

with I'_0, the resonance integral after subtracting the 1/v component. The G_{th} and G_{epi} denote the self-shielding coefficients for thermal and epithermal neutrons, respectively. Values of parameters are shown in Table in Ref. 77 for the flux monitors of this experiment. Noting that g and G_{th} are almost unity in this experiment, we took unity for gG_{th} in the analysis. From Eqs. (9) and (10), following two relations were deduced;

$$R/\sigma_0 = \phi_1 + \phi_2\, s_0 G_{epi} \tag{12}$$

for irradiation without a Cd shield,

$$R'/\sigma_0 = \phi'_1 + \phi'_2\, s_0 G_{epi} \tag{13}$$

for irradiation with a Cd shield,

where $\phi_{1,2}$ and $\phi'_{1,2}$ are determined for each irradiation by using values of R and R' for each monitor (Co/Al and Au/Al). It is not assumed that $\phi_2 = \phi'_2$. It was found that $\phi'_1/\phi_1 = 1/13$ and $\phi'_2/\phi_2 \fallingdotseq 1$.
Since the Eqs. (12) and (13) give the relation

$$s_0 G_{epi} = \frac{\phi_1 - \phi'_1(R/R')}{\phi_2 - \phi'_2(R/R')}, \tag{14}$$

the value of s_0G_{epi} for the reaction $^{137}Cs(n,\gamma)^{138}Cs$ is deduced from the value of R/R' for this reaction by taking unity for gG_{th} as for the neutron monitors. Then the value of σ_0 is obtained from Eq. (12). The value obtained for the thermal neutron capture cross section is 0.25 ± 0.02 b. This value is twice of the value reported by Stupegia[80] (0.110 ± 0.033 b). Since it is reasonable to assume that $G_{epi} = 1$; the value of s_0 can be obtained as 1.1 ± 0.3. By the definition of (11), the value of I'_0 is deduced. The results are

$$\sigma_0 = 0.25 \pm 0.02\ b, \quad \text{and} \quad I'_0 = 0.24 \pm 0.07\ b$$

The value of the resonance integral I_0 can be calculated by assuming the Cd cut-off energy. For the cut-off energy of 0.5 eV, I_0 is given by

$$I_0 = I'_0 + 0.45\sigma_0 \tag{15}$$

where $0.45\sigma_0$ is the 1/v contribution. The value of $I_0 = 0.36 \pm 0.07$ b. was obtained and this value is compared with the recent evaluation[81),82)].

6. 2 Measurement of Thermal Neutron Cross Section of the Reaction $^{90}Sr(n,\gamma)^{91}Sr$

The thermal neutron cross section of the reaction $^{90}Sr(n,\gamma)^{91}Sr$ has been measured[78)] by means of an activation method. Since the target nucleus(^{90}Sr) decays through the beta-decay and does not emit gamma-rays, the gamma-ray emitting activity ^{85}Sr was mixed in the ^{90}Sr sources and used for the tracer of Sr elements. The ratio of amount of ^{85}Sr and ^{90}Sr was measured in advance with the beta-ray and gamma-ray spectroscopic method. Strontium chloride target containing about 2 MBq of ^{90}Sr were irradiated for 10 min with reactor neutron of the reactor JRR-4 of JAERI. Activation detectors of Co/Al and Au/Al alloy wires were irradiated simultaneously to monitor the neutron flux and Westcott's epithermal index as was done for ^{137}Cs. The irradiated Sr samples were purified chemically and their gamma-ray spectra were measured with a high purity Ge detector with a large detection efficiency.

An effective cross section of the $^{90}Sr(n,\gamma)^{91}Sr$ reaction for a reactor neutron spectrum was determined from the ratio of radioactive elements, ^{91}Sr and ^{85}Sr (the ratio to the ^{90}Sr is known), and neutron flux data as was done for the cross section measurement of ^{137}Cs. The resonance integral was also measured by the modified Cd-ratio method. The value of the resonance integral obtained was too small and the upper limit was deduced. Considering an upper limit of the resonance integral to be 0.16 b, the thermal neutron cross section (for 2,200 m/s neutron) of $^{90}Sr(n,\gamma)^{91}Sr$ reaction was found to be

$$\sigma_0 = 0.0153 \pm \begin{matrix} 0.0013 \\ 0.0042 \end{matrix}$$

The value obtained is only 1/50 of the value reported by Zeisel[83)] and is in good agreement with the figure reported by McVey et al[84)].

7. Summary

Study of radioactive nuclides has been done at the Department of Nuclear Engineering. The radioactive nuclei were produced through nuclear reactions caused by various methods, such as fast neutron irradiation, thermal neutron irradiation, charged particle irradiation and gamma-ray irradiation. Chemical separation processes were applied sometimes to obtain pure samples. The on-line isotope separation methods were also used for the separation of nuclides from impurity nuclides. In case of short-lived nuclides, the produced nuclei were used for the measurement immediatly after the production. Beta-rays and gamma-rays from radioactive nuclides were measured to investigate the nuclear structure. New beta-rays and gamma-rays were observed. Decay schemes of short lived nuclei were determined from our works, many new levels were proposed and new data for the nuclear structure study were presented. The activation methods were used for the measurement of reaction cross sections. In most cases, reaction products are radioactive and the intensities of the radioactivities

indicate the amount of produced nuclei through the reaction. Therefore, we applied the activation methods for the measurement of the cross sections. The cross sections for 14 MeV neutrons were measured by using the 2 MeV Van de Graaff of Nagoya University, the Intense Neutron Facility of Osaka University and the Fast Neutron Source of Japan Atomic Energy Research Institute (JAERI). Measurements of thermal neutron cross sections for fission products were performed at JAERI. Results of these studies are shown in References.

Acknowledgments

A part of this work was carried out with the help by Messrs. Y. Tsurita and T. Masuda. Facilities of Research Reactor Institute, Kyoto University, OKTAVIAN (Intense Neutron Facility) at Osaka University, FNS (Fast Neutron Source) at Japan Atomic Energy Research Institute (JAERI), facilities of Research Reactor Institute, Rikkyo University, Research Reactors at JAERI, facilities of Institute for Nuclear Study, University of Tokyo, and facilities of Vanderbilt University, U.S.A., were used for this study. The authors are grateful to the staffs of these facilities.

References

1) Kawade, K., Yamamoto, H., Amemiya, S., Hiei, A., Katoh, T.: J. Nuclear Science & Technology, 10(8), pp.507–510 (1973).
2) Sumita, K., Takahashi, A., Iida, T., Yamamoto, J.: Nuclear Science & Engineering, 106, pp.249–265 (1990).
3) Amemiya, S., Itoh, M., Kawade, K., Yamamoto, H., Katoh, T.: J, Nuclear Science & Technology, 11(9), pp.395–402 (1974).
4) Okano, K., Kawase, Y., Kawade, K., Yamamoto, H., Hanada, M., Katoh, T.: Nuclear Instruments & Methods, 186, pp.115–120 (1981).
5) Kawade, K., Yamamoto, H., Amano, H., Hanada, M., Katoh, T., Okano, K., Kawase, Y., Fujiwara, I.: Nuclear Instruments & Methods, 200, pp.417–422 (1982).
6) Yoshizawa, Y., Iwata, Y., Kaku, T., Katoh, T., Ruan, J-Z., Kojima, T., Kawada, Y.: Nuclear Instruments & Methods, 174, pp.109–131 (1980).
7) Ritz, A., Bureau International des Poids et Mesures, BIPM-77/4 (1977).
8) Yoshizawa, Y., Iwata, Y., Katoh, T., Ruan, J-R., Kawada, Y.: Nuclear Instruments & Methods, 212, pp.249–258 (1983).
9) Morinaga, H., Takahashi, K., Nuclear Physics, 38, p.186 (1962).
10) Katoh, T.: J. Physical Society of Japan, 25(1), pp.51–53 (1968).
11) Wapstra, A. H. , et al.: Nuclear Spectroscopy Tables, p.71 (North-Holand Pub. Co. Amsterdam, 1959).
12) Brantley, W. H., Hamilton, J. H., Katoh, T., Zganjar, E. F.: Nuclear Physics, A118(3), pp.678–685 (1968).
13) Hamilton, J. H., Katoh, T., Brantley, W. H., Zganjar, E. F.: Physics Letteres, 13(1), pp.43–46 (1964).
14) Hamilton, J. H., Brantley, W. H., Katoh, T., Zganjar, E. F.: Internal Conversion Processes ed. by J. H. Hamilton p.297 (Academic Press, New York, 1966).
15) Brantley, W. H.: Ph.D. thesis, Vanderbilt University, U. S. A. (1966).
16) Hamilton, J. H., Manthuruthil, J.: Nuclear Physics, A118, (1968).